nagra
National Cooperative for the
Disposal of Radioactive Waste

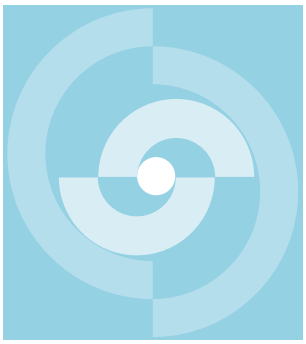

TECHNICAL REPORT 02-09

Assessment of Porewater Chemistry in the Bentonite Backfill for the Swiss SF/HLW Repository

December 2002

E. Curti, P. Wersin

Hardstrasse 73, CH-5430 Wettingen/Switzerland, Telephone +41-56-437 11 11

nagra
National Cooperative for the
Disposal of Radioactive Waste

TECHNICAL REPORT 02-09

Assessment of Porewater Chemistry in the Bentonite Backfill for the Swiss SF/HLW Repository

December 2002

E. Curti[1)], P. Wersin[2)]

[1)] Paul Scherrer Institut, Villigen PSI

[2)] Nagra, Wettingen

Hardstrasse 73, CH-5430 Wettingen/Switzerland, Telephone +41-56-437 11 11

This report was prepared on behalf of Nagra. The viewpoints presented and conclusions reached are those of the author(s) and do not necessarily represent those of Nagra.

PREFACE

The Laboratory for Waste Management of the Nuclear Energy and Safety Research Department at the Paul Scherrer Institut is performing work to develop and test models as well as to acquire specific data relevant to performance assessments of planned Swiss nuclear waste repositories. These investigations are undertaken in close co-operation with, and with the financial support of, the National Cooperative for the Disposal of Radioactive Waste (Nagra). The present report is issued simultaneously as a PSI-Bericht and a Nagra Technical Report.

ISSN 1015-2636

ABSTRACT

The porewater chemistry in the bentonite backfill will strongly affect the mobility of radionuclides via sorption and solubility equilibria. The aim of this study was to derive a reference bentonite porewater composition for the Swiss high-level waste repository and to estimate compositional uncertainties. Special emphasis was put on the evaluation of acid-base buffering mechanisms and the related variables pH and pCO_2.

Recent experimental data at high solid/water ratios are analysed by means of a classical aqueous solution - mineral equilibrium model using two distinct sets of constants for sorption reactions. An optimised thermodynamic model is then applied to repository conditions. A sensitivity analysis is then performed to identify critical geochemical parameters and to quantify their effect on porewater chemistry. The evolution of porewater chemistry in time is studied with the help of two alternative models, one based on water-exchange cycles, the other relying on diffusion. For the derivation of the reference porewater, a redox model based on the equilibrium between magnetite and dissolved Fe^{2+} is integrated in the clay/water reaction model. Uncertainties related to pH, Eh, and major anion concentrations (Cl^-, SO_4^{2-}, CO_3^{2-}) are evaluated. Finally, available trace element data are presented.

Two limiting bentonite porewater compositions with pCO_2 fixed at $10^{-3.5}$ and $10^{-1.5}$ bar have been modelled, which define the pH and Eh boundaries specified below. A third, intermediate composition, calculated with pCO_2 fixed at $10^{-2.2}$ bar, is considered to reflect the most probable repository conditions, and is thus defined as reference bentonite porewater. The resulting three waters are Na-(Ca-Mg-)-Cl-(SO_4) dominated and have a ionic strength of about 0.3 M.

The main results of this modelling study can be summarised as follows:

- The large uncertainty related to the pCO_2 in equilibrium with the groundwater permeating the host-rock has a significant effect on the pH of the bentonite porewater, resulting in a relatively wide range (from 6.9 to 7.8).
- Redox conditions are predicted to be reducing at all assumed pCO_2, resulting in oxidation potentials between -280 and -130 mV.
- The bentonite porewater chemistry is expected to remain stable over very long times, largely because of its similarity to the surrounding Opalinus Clay water.

Conventional thermodynamic models, as applied in this study and in other safety assessments, do not consider some complex physico-chemical processes occurring specifically in highly compacted, swelling clays (e.g. osmosis, reduction of external porosity). Further experimental investigations and new methodologies need to be developed to understand such processes and to integrate them in geochemical models. Nevertheless, we performed additional calculations with a refined model to account for the effects of anion exclusion and porosity reduction. The results indicate that porewater composition is quite insensitive to such processes. This makes us confident that the derived reference porewater composition is a reasonable estimate and is suitable for performance assessment.

ZUSAMMENFASSUNG

Die Porenwasserchemie der Bentonitverfüllung beeinflusst die Mobilität von Radionukliden über Sorptions- und Löslichkeitsgleichgewichte nachhaltig. Das Ziel dieser Arbeit war die Herleitung eines Referenzporenwassers für das schweizerische Lager für hochaktive Abfälle und die Abschätzung von Unsicherheiten bezüglich dessen Zusammensetzung. Dabei galt ein spezielles Augenmerk den Säure-Base-Pufferungsmechanismen und den damit zusammenhängenden Variablen pH und pCO_2.

Neuere Experimente, die bei hohen Feststoff-/Wasserverhältnissen durchgeführt wurden, werden mittels eines klassischen chemischen Gleichgewichtsmodells und zwei unterschiedlichen Datensätzen von Sorptionsreaktionen ausgewertet. Ein optimiertes thermodynamisches Modell wird hierauf für Lagerbedingungen mit Hilfe der geochemischen Codes MINSORB und PHREEQC angewendet. Zudem wird eine Sensititivitätsanalyse durchgeführt, um die kritischen geochemischen Parameter zu identifizieren und deren Auswirkung auf die Porenwasserchemie zu quantifizieren. Die zeitliche Entwicklung der Porenwasserzusammensetzung wird mit Hilfe von zwei Modellen, das eine basierend auf Wasseraustauschzyklen, das andere auf Diffusion, verfolgt. Für die Herleitung des Referenzporenwassers wird ein Redoxmodell, das auf dem Gleichgewicht zwischen Magnetit und gelöstem Fe^{2+} basiert, in das Ton-/Wasser-Reaktionsmodell integriert. Unsicherheiten bezüglich pH, Eh und den Hauptanionen (Cl^-, SO_4^{2-} und CO_3^{2-}) werden evaluiert. Schliesslich werden vorhandene Daten von Spurenelementen präsentiert.

Zwei limitierende Bentonitporenwasserzusammensetzungen werden unter der Bedingung von fixiertem $pCO_2 = 10^{-3.5}$ bzw. $10^{-1.5}$ bar modelliert, um die Bandbreiten bezüglich pH und Eh zu definieren. Eine dritte intermediäre Zusammensetzung, die unter der Bedingung von $pCO_2 = 10^{-2.2}$ bar berechnet wurde, widerspiegelt die wahrscheinlichsten Lagerbedingungen und wird deshalb als Referenzwasser definiert. Alle resultierenden Wässer sind Na(-Ca-Mg)-Cl(-SO_4) dominiert und haben eine Ionenstärke von ca. 0.3 M.

Die wichtigsten Ergebnisse dieser Modellierungsstudie lassen sich wie folgt zusammenfassen:

- Die grosse Unsicherheit bezüglich des CO_2-Partialdrucks im Wirtgestein hat signifikante Auswirkungen auf den pH des Bentonitporenwassers, was eine relativ grosse Bandbreite (6.9 bis 7.8) zur Folge hat.
- Die Redoxbedingungen sind gemäss unseren Modellrechnungen für alle pCO_2-Bedingungen reduzierend; die daraus abgeleiteten Oxidationspotentiale sind im Bereich von -280 und -130 mV.
- Es wird erwartet, dass die Chemie des Bentonitporenwassers über lange Zeiträume stabil bleiben wird, was vor allem an seiner Ähnlichkeit mit dem umgebenden Porenwasser des Opalinustons liegt.

In konventionellen thermodynamischen Modellen, wie in dieser Arbeit und anderen Sicherheitsanalysen angewendet, werden einige komplexe physikalisch-chemische Prozesse, die in hochkompaktierten quellenden Tonsystemen vorkommen (z.B. Osmose, Reduktion der externen Porosität), nicht berücksichtigt. Weitere experimentelle Untersuchungen und neue methodische Arbeiten müssen für das Verständnis über diese Prozesse und deren Integration in geochemische Modelle entwickelt werden. In einem ersten Schritt haben wir ein etwas verfeinertes Modell angewendet, um Anionenausschlusseffekte und Porositätsreduktion zu berücksichtigen. Gemäss den Ergebnissen verändert sich dadurch die Porenwasserzusammensetzung nicht signifikant. Dies ist ein weiterer Hinweis darauf, dass die hergeleiteten Porenwasserzusammensetzungen realistisch sind und eine brauchbare Grundlage für die Sicherheitsanalyse darstellen.

RÉSUMÉ

La composition des eaux interstitielles dans le remplissage de bentonite influe de manière importante sur la mobilité des radionucléides par le biais des phénomènes de solubilité et de sorption. L'objectif de cette étude était d'obtenir une composition de référence pour les eaux interstitielles de la bentonite utilisée dans le dépôt suisse pour déchets de haute activité et d'estimer les incertitudes relatives à cette composition. Les mécanismes de tamponnage acide-base et les variables correspondantes – pH et pCO_2 – ont fait l'objet d'une attention particulière.

Des données provenant d'expériences récentes effectuées à des rapports élevés solide/eau ont été analysées par le biais d'un modèle d'équilibre chimique classique en utilisant deux ensembles de constantes différents pour les réactions de sorption. Un modèle thermodynamique optimisé a ensuite été appliqué aux conditions du dépôt. On a de plus effectué une analyse de sensibilité pour identifier les paramètres géochimiques critiques et quantifier leur effet sur la composition de l'eau interstitielle. L'évolution dans la durée de la composition de l'eau est étudiée à l'aide de deux modèles différents, l'un basé sur les cycles d'échange d'eau, l'autre sur le processus de diffusion. Pour déduire la composition de référence, un modèle redox basé sur l'équilibre entre la magnétite et le Fe^{2+} dissous a été intégré au modèle de réaction argile/eau. Les incertitudes relatives aux pH, Eh, et aux principales concentrations d'anions (Cl^-, SO_4^{2-}, CO_3^{2-}) ont été estimées. L'étude présente enfin les données disponibles sur les éléments traces.

Deux compositions extrêmes ont été modélisées, avec un pCO_2 fixé respectivement à $10^{-3.5}$ et $10^{-1.5}$ bar, ce qui a fourni les limites nécessaires pour les pH et Eh. Une troisième composition, calculée pour un pCO_2 intermédiaire fixé à $10^{-2.2}$ bar, est censée représenter les conditions les plus probables régnant dans le dépôt. Elle est par conséquent définie comme la composition de référence de l'eau interstitielle. Les trois compositions sont de type Na-(Ca-Mg-)-Cl-(SO_4) et ont une force ionique d'environ 0.3 M.

Les principaux résultats de cette étude de modélisation peuvent être résumés de la façon suivante:

- L'incertitude importante relative aux valeurs de pCO_2 dans la roche d'accueil influe de manière considérable sur le pH de l'eau interstitielle de la bentonite avec, en conséquence, un large spectre de valeurs (entre 6.9 et 7.8).
- Selon les calculs effectués, les conditions redox sont réductrices à tous les pCO_2 envisagés et entraînent des potentiels d'oxydation situés entre -280 et -130 mV.
- La composition des eaux interstitielles restera probablement stable sur de longues périodes, en particulier du fait de sa similarité avec les eaux contenues dans les argiles à Opalinus environnantes.

Les modèles thermodynamiques conventionnels, tels qu'ils sont appliqués dans cette étude et dans d'autres études d'analyse de la sûreté, ne prennent pas en compte certains processus physico-chimiques complexes propres aux argiles gonflantes fortement compactées (par exemple l'osmose ou la réduction de la porosité externe). D'autres expériences et le développement de nouvelles méthodologies sont nécessaires pour comprendre ces processus et les intégrer aux modèles géochimiques. Nous avons toutefois effectué des calculs complémentaires avec un modèle affiné, de façon à prendre en compte les effets de l'exclusion des anions et de la réduction de la porosité. Les résultats montrent que ces processus ne modifient pas la composition des eaux interstitielles de manière significative. Ceci nous permet d'avancer que la composition de référence des eaux interstitielles obtenue constitue une base de travail réaliste, pouvant être utilisée dans le cadre d'une analyse de la sûreté.

TABLE OF CONTENTS

LIST OF TABLES

LIST OF FIGURES

1 INTRODUCTION

The long-term chemical stability of the water-saturated bentonite backfill is an important safety requirement for high-level waste disposal. It is essential to have a detailed knowledge on the equilibrium composition of the bentonite porewater, since it controls solubility and sorption of radionuclides and affects the corrosion of the steel canister containing the waste. At present, the determination of porewater chemistry in the near field still constitutes a difficult task, mainly because of the incomplete understanding of the chemical and physical properties in compacted bentonite.

The study of bentonite porewater chemistry has been an integral part of Nagra's and PSI's research program for the last 15 years. WANNER (1986) developed a thermodynamic model, which to our knowledge included for the first time ion exchange processes. Based on experimental data by BATEMAN et al. (1991) CURTI (1993) extended this model by taking into account alumosilicate precipitation-dissolution reactions. Since then, extensive experimental and modelling work on montmorillonite - water interactions has been carried out (e.g. WIELAND et al., 1994; BAEYENS and BRADBURY, 1995; BRADBURY and BAEYENS, 1995, 1997, 1998, 2002a; MUURINEN and LEHIKOINEN, 1999; BRUNO et al., 1999), providing new insight into the processes controlling the chemistry of bentonite porewaters. Main improvements achieved in the last few years include:

- the integration of surface complexation reactions
- a better characterisation of accessory minerals
- refined thermodynamic constants for sorption reactions
- new experimental data at high solid/water ratios (up to 1500 g/L)

These improvements enable a more adequate thermodynamic treatment of the bentonite - water interactions, although we are well aware that current modelling approaches still neglect important, but poorly understood, effects related to compaction (e.g. osmosis, anion exclusion, swelling). The time-dependent modelling of bentonite porewater evolution is inflicted with even higher conceptual uncertainty (ANDERSSON, 1999), largely because of the poorly known physico-chemical processes in compacted clays. So far, only very crude time-dependent models, such as the water exchange cycle model (WANNER, 1986; WANNER et al., 1992; WIELAND et al. 1994; BRUNO et al., 1999) and very simplified diffusion-reaction models (ARCOS et al., 2000a; 2000b) have been applied. A summary of the different approaches used in recent safety assessment studies is given in Table 1.1.

The goal of this work is to derive a reference porewater composition and expected chemical variations for Na-bentonite surrounded by Opalinus Clay. The following procedure has been adopted:

1. Selection and evaluation of recent experimental data and modelling approaches.
2. Modelling of experimental data at high solid/water ratio with two alternative sets of thermodynamic constants (WIELAND et al., 1994; BRADBURY and BAEYENS, 1995).
3. Extrapolation to repository conditions with an optimised thermodynamic model including a sensitivity analysis.
4. Estimation of porewater evolution in time with two simple modelling approaches.
5. Definition of reference bentonite water and expected variations.
6. Evaluation of the effects of anion exclusion and porosity reduction on porewater composition (refined model, see Appendix E).

Table 1.1: Modelling approaches in recent safety assessments for estimating porewater chemistry in the near field.

Organisation / reference	**Safety assessment**	**Modelling approach for static situation**	**Model for evolution of porewater**
Nagra (1994)	Kristallin-I	ion exchange (no surface complexation), various silicate equilibria (CURTI, 1993)	qualitative evaluation (CURTI, 1993)
AECL (1994)	Vault model	ion exchange (no surface complexation) (LEMIRE and GARISTO, 1989)	water exchange (LEMIRE and GARISTO, 1989)
JNC (1999)	H-12	ion exchange and surface complexation (ODA et al., 1999)	water exchange (WANNER, 1986)
Posiva (1999)	TILA-99	no details given	not explicitly mentioned
SKB (1999)	SR 97	ion exchange and surface complexation (BRUNO et al., 1999)	water exchange (BRUNO et al., 1999)

2 GEOCHEMICAL CONDITIONS IN THE BENTONITE BACKFILL

2.1 Relevant processes

2.1.1 General aspects

The geochemistry of the bentonite backfill in a geological repository (Opalinus Clay in this case), is affected by a number of processes, some of which have been extensively investigated in laboratory, field or modelling studies (e.g., GRAUER, 1986; GRAUER, 1990). Key issues are the chemical stability and the buffering capacity of bentonite with regard to processes that affect its acid-base or redox properties. Another important issue is the swelling capacity, which may be adversely affected if significant amounts of montmorillonite have reacted to form other minerals.

The processes considered in our porewater model are schematically shown in Figure 2.1. These can be roughly classified into three categories: fast chemical reactions, slow chemical reactions, and diffusive processes.

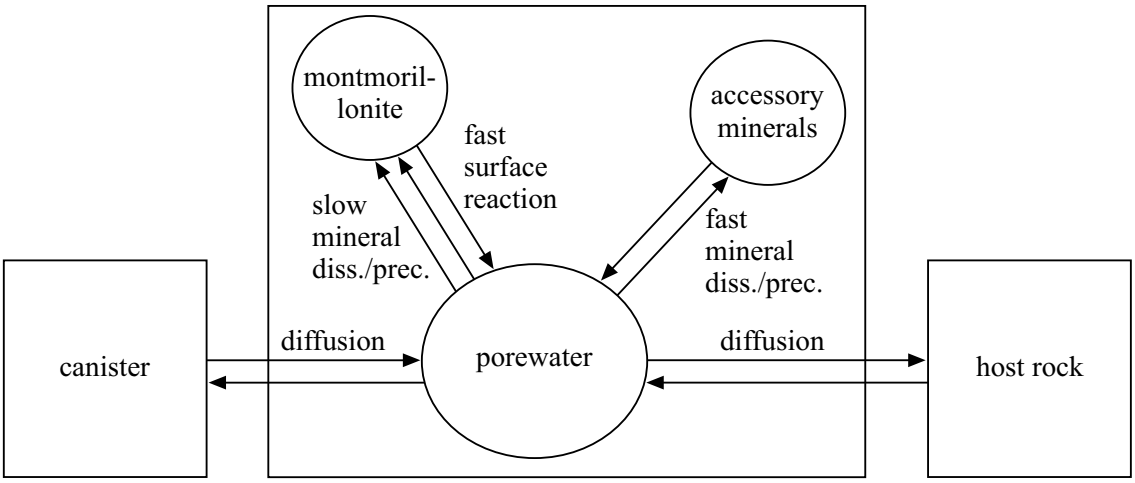

Figure 2.1: Processes affecting porewater chemistry in the bentonite backfill.

Fast chemical reactions

These are reversible processes that rapidly reach equilibrium (within minutes, hours or days). Examples are complexation in solution, surface reactions at clay surfaces, dissolution/ precipitation of accessory minerals (carbonates, oxides, sulphates) and dissolution of soluble salts (e.g. NaCl).

Sorption on montmorillonite takes place at two fundamentally different types of surface sites. The first site type (denoted as =Z in this report) arises from the permanent negative charge of the montmorillonite octahedral layer and leads to ion exchange processes. The second type (denoted as =XOH) are surface functional groups analogue to those of oxide mineral surfaces. These sites (often termed "edge sites") are characterised by strongly pH dependent sorption due to protonation and deprotonation of the terminal hydroxyl groups (e.g., WANNER et al., 1994).

BRADBURY and BAEYENS (1997) studied systematically the protonation/deprotonation of hydroxyl groups in purified MX-80 Na-montmorillonite by the batch titration technique. They were able to distinguish two sites with different capacity and affinity ("strong" and "weak" sites). With the help of the derived intrinsic constants, sorption edges of trace metals (Zn, Ni) could then be modelled successfully.

Slow chemical reactions

These are kinetically controlled reactions that are potentially relevant to porewater chemistry and are characterised by very long equilibration times. Examples are dissolution and precipitation reactions of silicate minerals. Relevant to repository safety are the transformation of montmorillonite to illite and silica (observed in natural analogue studies) and the possible transformation of montmorillonite to iron-rich silicates (e.g., nontronite, berthierine) close to the steel canister (e.g. GRAUER, 1990; 1993). The effect of illitisation and precipitation of silica has been evaluated for the bentonite backfill surrounded by Opalinus Clay (NAGRA 2002, BENBOW et al., 2000). The main conclusion drawn from these studies is that these processes will not adversely affect the long-term chemical stability of the bentonite. Because of the large acid-base and redox buffering capacity of bentonite, the chemistry of the porewater will not be significantly affected by minor transformation processes in the silicate mineralogy (GRAUER, 1993). The extent of transformation due to interaction with iron corrosion products is poorly known due to the lack of experimental data. This aspect needs to be considered in future safety assessments.

Diffusive processes

Diffusion is the dominant transport process in bentonite. A number of diffusion studies on compacted bentonite (e.g., SATO et al., 1992; 1995; CHOI and OSCARSON, 1996), most of which investigated transport of radionuclides, have been performed. The results indicate a large range of apparent diffusion coefficients, due to strong variations in retardation, mainly attributed to differences in sorption distribution coefficients (YU and NERETNIEKS; 1997 SATO and YUI, 1997; SATO, 1998). The diffusion-accessible porosity appears to be smaller for anions than for cations and neutral species. This has been explained by ion exclusion effects arising from the electric double layer of the negatively charged clay surfaces. (cf. next section). For cations such as Na^+ and Ca^{2+} an additional diffusive flux at the clay surfaces, termed surface diffusion, has been proposed (YU and NERETNIEKS, 1997), although the significance of such a process is highly controversial (OSCARSON, 1994).

Recently, the relations between the sorption of trace radionuclides and their diffusion properties in compacted bentonite were studied. Starting from batch experiment data obtained in diluted montmorillonite suspensions, BRADBURY and BAEYENS (2002b) calculated distribution coefficients for Cs(I), Ni(II), Am(III), Sm(III), Zr(IV) and Np(V) as a function of dry density (up to 2000 kg m^{-3}) for "Kunigel V1" bentonite. They then compared the calculated distribution coefficients (K_d) with those directly derived from diffusion experiments. Although the calculations required taking into account the effects of pH, porewater speciation and mineralogy (owing to the differences between the materials and conditions in the batch experiments and those in the diffusion experiments) the K_d values calculated from the batch experiments were found to agree surprisingly well with those inferred from the diffusion experiments over a wide range of S/W ratios. On the other hand, as pointed out by the authors, the comparison between batch and diffusion K_d values for some other redox sensitive radioelements (U, Pu, Tc), revealed significant differences.

In spite of these rather encouraging results, diffusive processes in compacted clays are still not well understood. The effects of a variety of physical and chemical parameters, in particular the solid/water ratio (S/W), salinity, microstructure of the pores, charge and dimension of the diffusing ion have to be separated and elucidated. So far, a coherent diffusion model for compacted bentonite, based on the mechanistic understanding of all physico-chemical factors listed above is lacking. Thus, diffusion is commonly treated by a simple Fickian model assuming a homogenous medium. This approach was also adopted here for the assessment of time-dependent porewater evolution (chapter 4).

Effect of compaction

Due to the specific property of montmorillonite to swell during water uptake, a large fraction of the aqueous phase will reside in the structural interlayer separating the tetrahedral-octahedral-tetrahedral units of the clay platelets (see Figure B-1, Appendix B). This water is denoted "interlayer water" in contrast to the remaining "external water" which will be located in pores between the mineral particles (Figure 2.2). In compacted clay, the physical and chemical properties of both interlayer and external porewater may be significantly altered compared to a dilute system (e.g., GRAUER, 1986). This is for example indicated by diffusion data and squeezing experiments at high S/W ratio, which point to ion exclusion effects (MUURINEN and LEHIKOINEN, 1999). Because of the difficulty to obtain reliable experimental data in highly compacted clays, there is, to our knowledge, no model available to describe such effects satisfactorily. Clay-water interactions are treated conventionally in this study, and thus no distinction is made between the properties of interlayer and external porewater. This aspect is discussed in more detail in Appendix D. An extended model that takes some of these aspects into account is presented in Appendix E.

2.1.2 Indications from experimental data

A number of experimental studies on bentonite-water systems has been performed. Table 2.1 summarises results of equilibration experiments performed with MX-80 bentonite by SNELLMAN et al. (1987), MELAMED et al. (1992), WERME (1992) and MUURINEN and LEHIKOINEN (1999). The experiments on Avonlea bentonite (OSCARSON and DIXON, 1989), Spanish bentonite (CUEVAS et al., 1997) and on Montigel bentonite (BATEMAN et al., 1991; 1996) are also noteworthy in this context. A compilation of the data (Table 2.1), which reflect a large range of conditions, allows us to explore major trends, e.g. with regard to changing S/W or to the composition of the initial solution.

Chloride, sulphate

The concentrations of these ions are highly variable and strongly reflect the salinity of the added solution (Table 2.1, e.g. data of MUURINEN and LEHKOINEN, 1999). The solution concentrations also depend on the S/W ratio; with increasing S/W a linear increase is observed for both ions. This indicates the presence of soluble salts in the bentonite, such as $CaSO_4$ and NaCl (WANNER et al., 1992). At high S/W ratio the squeezing experiments of MUURINEN and LEHIKOINEN (1999) indicate chloride and sulphate concentrations consistently lower than in equilibration experiments carried out in more diluted suspensions (data not shown here), which points to ion exclusion effects.

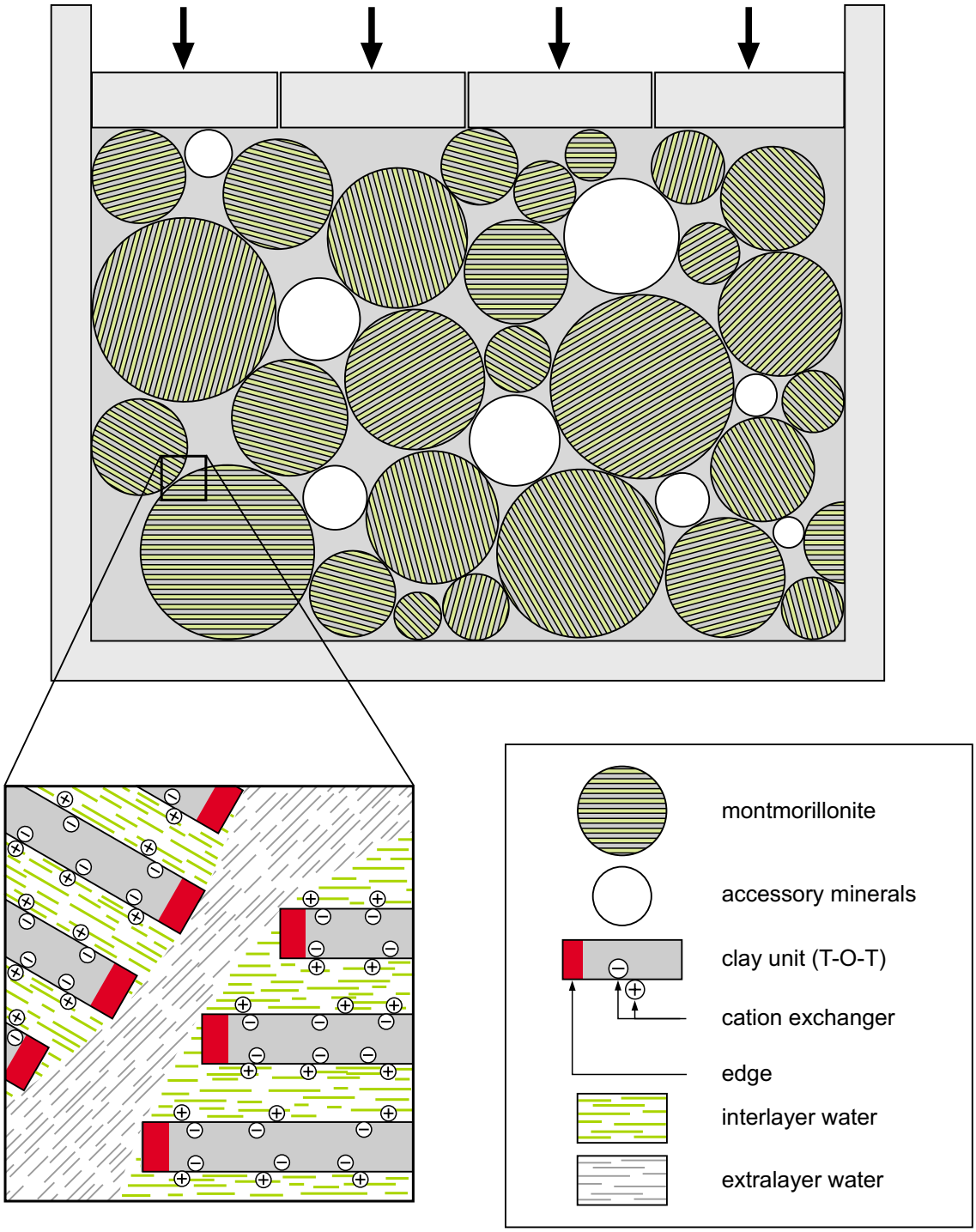

Figure 2.2: Schematic presentation of microstructure in compacted bentonite. Provided by the courtesy of B. Schwyn.

Sodium, calcium, magnesium, potassium

The concentrations of major cations (Na^+, Ca^{2+}, Mg^{2+}, K^+) also depend on the salinity of the added solution and the S/W ratio, however there is no linear dependency on the S/W ratio as noted for major soluble anions, since these cations participate to cation exchange or dissolution/precipitation reactions. In all experiments Na^+ is the dominant cation in solution (about 5 - 500 mmol/L). Calcium concentrations are consistently lower. The observed pattern has been explained by calcite equilibrium and ion exchange between Na^+ and Ca^{2+} (e.g., WANNER et al., 1992):

$$2NaZ + CaCO_3 + H^+ \Leftrightarrow CaZ_2 + 2Na^+ + HCO_3^-$$

where NaZ and CaZ_2 denote Na and Ca exchanged species.

Mg-concentrations are rather variable (about 0.1-10 mmol/L), but generally lower than for Ca. K-concentrations originating from the bentonite are generally low (< 3 mmol/L).

Carbonate

Under the conditions imposed in the experiments bicarbonate is the dominant carbonate species and occurs at millimolar concentrations. In general, carbonate concentrations are controlled by calcite equilibrium and pCO_2 (e.g. SNELLMAN et al. 1987; CURTI, 1993).

Silica

Observed Si-concentrations (data not shown) are variable, but usually below 1 mmol/L. They have been explained by quartz (WANNER et al., 1992) or kaolinite/gibbsite saturation equilibrium (CURTI, 1993).

pH

Figure 2.3 summarises measured pH values determined from MX-80 studies and other bentonites. The pH range for all data is 7.2 to 9.4 with no systematic correlation as a function of the S/W ratio. There is a trend in the data of MUURINEN and LEHIKOINEN (1999) (Table 2.1) and BATEMAN et al. (1996) indicating a decrease in pH with increasing ionic strength.

Equilibrium model

The experimental data can be reasonably described in terms of a simple equilibrium model which includes calcite saturation, a fixed pCO_2, ion exchange reactions and dissolution of soluble salts, such as NaCl, $CaSO_4$ (e.g. WANNER, 1986; WANNER et al., 1992; WIELAND et al., 1994; BRUNO et al., 1999). This appears to hold also for data obtained at higher temperature (CUEVAS et al., 1997). At high S/W, however, the agreement between experiments and modelling is not always satisfactory. This may arise from neglecting protonation-deprotonation reactions on edge sites or from the previously mentioned, poorly understood effects specific to compacted bentonite systems (e.g. ion exclusion).

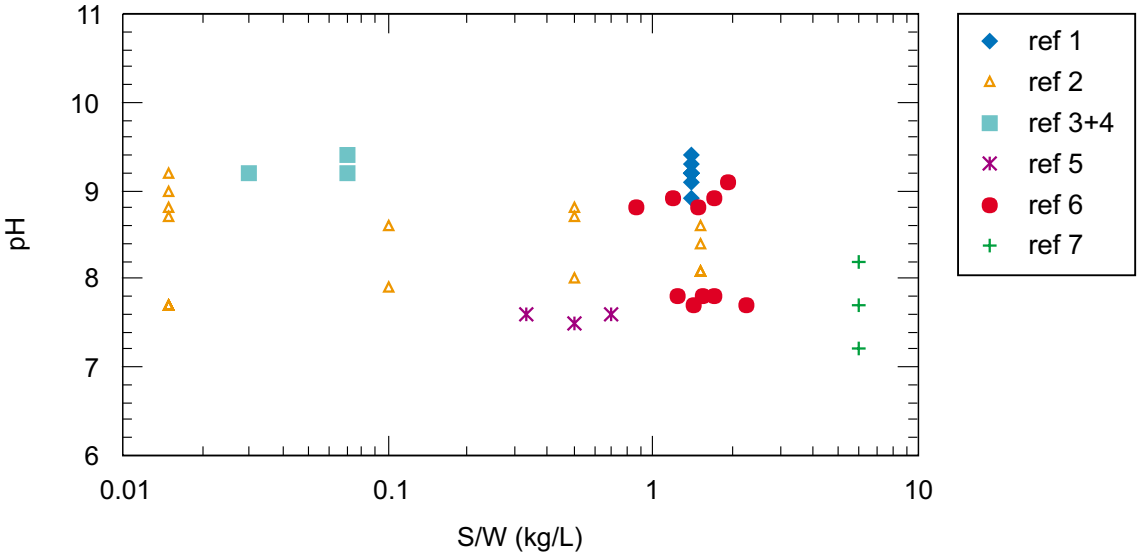

Ref. 1: WERME (1992), unpublished data presented in WANNER et al. (1992)
Ref. 2: MUURINEN and LEHIKOINEN (1999)
Ref. 3: SNELLMAN et al. (1987)
Ref. 4: MELAMED et al. (1992)
Ref. 5: OSCARSON and DIXON (1989)
Ref. 6: BATEMAN et al. (1996)
Ref. 7: CUEVAS et al. (1997)

Figure 2.3: Measured pH values vs. solid/water ratios from bentonite batch experiments.

2.1.3 Indications from natural analogues

The closest natural analogues of compacted bentonites are mudstones and shale formations. Unfortunately, there are only very few reliable data available on porewaters from such rocks. Of interest in this context are recent data from the Opalinus Clay at Mont Terri (e.g. DEGUELDRE et al., 2003; PEARSON et al., 1999) and from the Boom clay (BEAUCAIRE et al., 2000). Also these porewaters (Table 2.1) can be reproduced reasonably well by chemical equilibrium models (PEARSON et al., 1999; BEAUCAIRE et al., 2000) similar to those commonly used for bentonite systems.

Table 2.1: Summarised results from bentonite batch experiments and porewater compositions of two clay formations.

Reference	**Bentonite**	**S/W** (kg/dm^3)	**T** (°C)	**initial I** (mol/L)	**pH**	**Na** (mmol/L)	**Ca** (mmol/L)	**Mg** (mmol/L)	**K** (mmol/L)	**HCO_3** (mmol/L)	**SO_4** (mmol/L)	**Cl** (mmol/L)	**Si** (mmol/L)
Snellman et al. (1987)	MX-80	0.03	room T	0.0045	9.2	11	0.28	0.15	0.07	6.6	0.06	1.9	0.25
Melamed et al. (1992)	MX-80	0.07	70	0.004 0.4	9.2 9.4	11.7 19.9	0.07 0.06	0.03 0.008	0.14 3.2	4.0 4.2	2.6 2.6	1.6 11.7	0.40 0.34
Muurinen and Lehikoinen (1999)	MX-80	0.015 -1.5 "	room T "	0.004 0.42	8.6 - 9.9 7.7 - 8.8	4 - 247 181 - 522	0.2 - 9.0 39 - 94	0.2 - 2.4 2.2 - 14	0.13 - 3.7 0.14 - 4.7	1.6 - 7.0 0.3 - 2.7	0.7 - 129 0.4 - 34	1.7 - 11.7 398 - 466	0.2 - 0.7 0.14 - 4.0
Werme (1992)	MX-80	1.4	room T	0 + 0.004	8.9 - 9.4	70 - 110	0.2 - 5.0	<0.01 - 0.04	n.d.	3.3 - 12	29 - 43	1.5 - 2.0	n.d.
Oscarson and Dixon (1989)	Avonlea	0.3 - 0.7	room T	0	7.5 - 7.6	61 - 117	2.8 - 8.6	0.6 - 1.9	0.5 - 0.8	1.7 - 2.3	32 - 66	4.7 - 10.3	n.d.
Bateman et al. (1991; 1996)	$NaCO_3$-Montigel	0.9 - 1.9 1.2 - 2.3	50	0.013 0.2	8.9 - 9.1 7.7 - 7.8	42 - 65 223 - 370	0.01 - 1.2 0.07 - 0.4	<0.01 - 1.2 0.7 - 0.9	0.1 - 0.7 0.5 - 0.9	11 -28 7.8 - 11	2.4 - 3.9 2.8 - 3.3	19.8 - 24.9 229 - 301	n.d "
Cuevas et al. (1997)	Spanish bentonite	~ 6	25 65 - 72	0 "	7.2 7.7 -8.2	105 50 -104	14.3 2.1 -7.0	45.3 4.0 - 12	0.3 0.7 -2.4	2.8 2.9 -4.2	15.5 11 -28	185 46 -93	0.2 n.d.
	Clay rock												
Degueldre et al. (2003)	Opalinus Clay, Mt. Terri	~ 24	14		7.4 - 7.9	120 - 240	7-15	6-16	1.1-1.5	1-5	11-15	130-270	0.08 - 0.11
Beaucaire et al. (2000)	Boom clay, Mol				8.2 - 8.8	12.6	0.05	0.1	0.2	12	0.04	0.5	0.2

2.2 Redox conditions

Redox conditions in the backfill will depend to a large extent on corrosion processes of the canister and on the supply of redox sensitive species from the surrounding host rock. The concentrations of redox sensitive phases in bentonite is low (minor Fe(II) and Fe(III)-minerals) and some of these may not react at low temperatures. To date there is no direct experimental information on redox buffers in such a complex environment. For instance, the role of montmorillonite itself as redox-sensitive phase is not clear. Therefore, we have estimated redox conditions using indirect experimental evidence and simple chemical concepts, developed in a separate note (WERSIN et al., 2003). The essential results of this work are presented here briefly:

- After a short initial oxic phase (consumption of trapped oxygen), reducing conditions in the bentonite backfill will be established.
- The oxidation potential will be largely determined by the corrosion of steel, resulting in large amounts of magnetite, and by the reducing conditions of the surrounding Opalinus Clay.
- The oxidation potential (Eh) will be strongly coupled to pH. Based on a number of arguments, it is suggested to estimate Eh from the magnetite equilibrium and dissolved Fe(II).

The redox concept of WERSIN et al. (2003) is integrated in the geochemical model applied for the derivation of the bentonite reference water (chapter 5).

2.3 Conventional thermodynamic models for clay-water interactions

Models predicting clay-water chemical interactions are mostly based on equilibrium thermodynamics and implemented in conventional geochemical codes (PHREEQC, MINSORB, EQ3/6). Historically two approaches can be distinguished:

a) **Solid solution models**, in which clay minerals are treated as multipole ideal solid solutions. In this approach, followed for example by a school of French clay mineralogists (TARDY and FRITZ, 1981; TARDY and DUPLAY, 1992), clay minerals are regarded as rapidly reacting solids, which change composition (including the structural tetrahedral-octahedral units) as a function of the composition of the contacting solution. An empirical solid solution approach has been adopted by MATTIGOD and SPOSITO (1978) where standard thermodynamic properties of clays are estimated from their oxide or hydroxide components. Typically, surface reactions are neglected in solid solution models.

b) **Sorption models**, adopted in the present study (WANNER, 1986; WANNER et al., 1992; CURTI, 1993; WIELAND et al., 1994; BRUNO et al., 1999; ARCOS et al., 2000a) which rely on a detailed description of ion exchange and surface complexation reactions. In this modelling approach, the tetrahedral-octahedral-tetrahedral (TOT) sheet units of the clay minerals are regarded as essentially inert (insoluble) at the low temperatures of interest.

In principle, both approaches should be integrated taking account of the different kinetics of the reactions involved, but the question of the timescales and temperatures required for the formation of solid solutions in clay minerals is still unresolved (GRAUER, 1990). Also, end-member solubility data for clays are still scarce and controversial (e.g. MAY et al., 1986). For these reasons, surface adsorption models are generally preferred for safety assessment purposes.

3 MODELLING INITIAL POREWATER IN THE SATURATED BACKFILL

3.1 Introductory remarks

In this chapter, we develop a method to derive bentonite porewater compositions reflecting the conditions prevailing in the repository soon after resaturation and consumption of trapped oxygen. The porewaters have been modelled with the help of conventional geochemical codes (MINSORB and PHREEQC) using state-of-the-art thermodynamic data. Chemical processes considered include gas exchange (CO_2), complexation reactions in solution, cation exchange for Na^+, K^+, H^+, Mg^{2+}, Ca^{2+} and Sr^{2+}, surface complexation reactions (protonation/deprotonation, Mg^{2+}, Ca^{2+}), saturation equilibria for reactive minerals (calcite, gypsum, quartz, kaolinite) and dissolution of soluble salts (NaCl). Figure 3.1 shows schematically the modelled bentonite-water system with the main reactions considered.

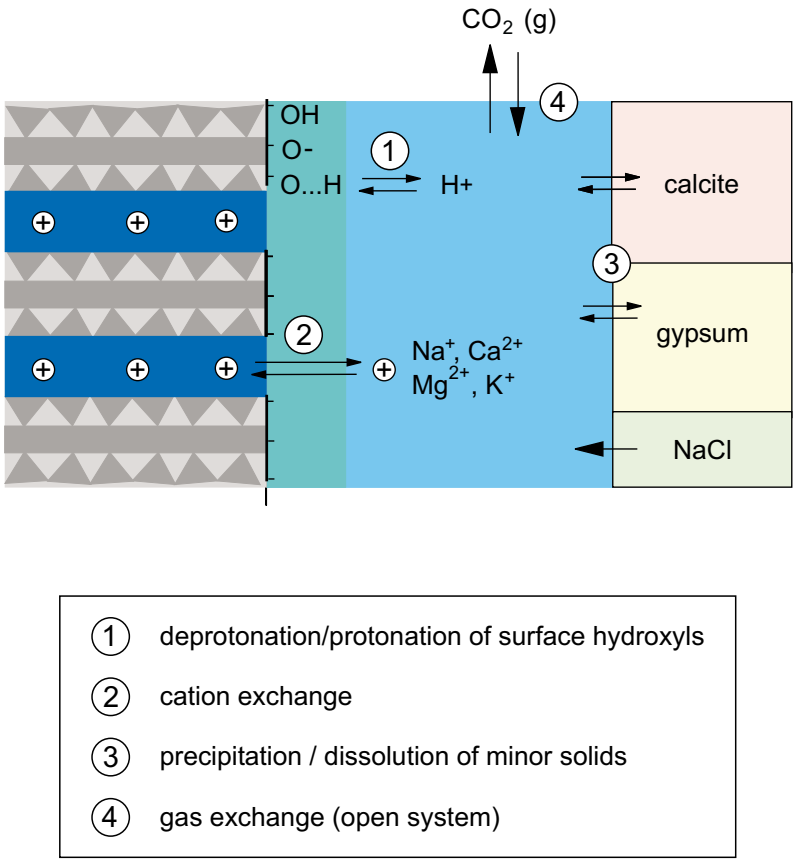

Figure 3.1: Sketch showing the bentonite-water system as modelled in this report. Blue colours refer to the various water types discussed: interlayer water (dark blue), DDL water (cyan) and uncharged external porewater (middle blue).

Although the model has been successfully tested against the results of recent water-bentonite interaction experiments conducted at S/W ratios as high as 1.5 kg/L (see section 3.2), application to realistic repository conditions requires extrapolation to even higher compaction degrees (S/W = 4.5 kg/L). Some physico-chemical processes and effects occurring in such

highly compacted clay systems are currently poorly known and were therefore not considered in our model (see section 2.3 and Appendix C). It was assumed that chemical interactions within a compacted water-saturated bentonite could be represented by conventional mass action models as for clay suspensions and semi-compacted systems.

3.2 Properties of MX-80 bentonite and Opalinus Clay water

MX-80 Na-bentonite from Wyoming, USA (supplied by Bentonite International GmbH, D-41 Duisburg - Meiderich) was selected as a reference material for our model calculations. This material has been thoroughly characterised in preceding studies, so that mineralogical composition, cation exchange properties and surface site densities are well known. We relied on the recent characterisation work of BRADBURY and BAEYENS (1997, 1998, 2002a), which largely confirms the previous findings of MÜLLER-VONMOOS and KAHR (1983).

In the model, we assume that the bentonite reacts with reference Opalinus Clay water (composition given by PEARSON, 2002). The relevant material properties of MX-80 bentonite and the composition of the reference Opalinus Clay water are listed in Table 3.1 along with other model parameters.

The S/W ratio of 4.5 kg/L was derived from the bulk densities of dry and saturated bentonite (ρ_{dry} and ρ_{wet}, respectively) as given by JOHNSON and SCHNEIDER (2000) assuming a water density ρ_w of 1 kg/L:

$$S/W = \rho_w \frac{\rho_{dry}}{\rho_{wet} - \rho_{dry}} = 1 \times \frac{1711.2}{2091.2 - 1711.2} = 4.5 \quad kg/L$$

This results in a "porosity" $\varepsilon = 0.38$, assuming a lattice density $\rho_s = 2.76$ kg/L:

$$\varepsilon = \frac{\rho_s}{\rho_s + (S/W)} = \frac{2.76}{2.76 + 4.5} = 0.38$$

Little is known about the pCO_2 in equilibrium with the Opalinus Clay water, so this critical parameter is presently highly uncertain. PEARSON (2002) gives a range of possible partial pressures between $10^{-3.5}$ and $10^{-1.5}$ bar and a reference value of $10^{-2.2}$ bar. The latter pressure, which we adopt as fixed boundary condition for the bentonite porewater model, is based on direct analyses of Benken core samples, corrected to account for microbial CO_2 production. The boundaries given above for the CO_2 partial pressure will be considered in the sensitivity analysis (see section 3.5.4).

Surface site concentrations (in equivalents per kg dry bentonite) were taken from the detailed characterisation work on purified Na-montmorillonite of BRADBURY and BAEYENS (1997). Note that, although these authors distinguish three site types (necessary to model trace metal sorption), two of them are sufficient to describe the protonation/deprotonation of hydroxyl surface sites considered in our model.

In Table 3.1, a BET surface area of 31300 $m^2\ kg^{-1}$ is reported. This quantity refers to the total external surface area accessible to N_2 gas sorption, which includes the area contributed by both montmorillonite and minor oxide minerals. In contrast, surface site concentrations are given in equivalents per kg of pure montmorillonite. Since both quantities were combined to calculate the site density in equivalents per m^2, an inconsistency is introduced. However, if the surface site concentrations were normalised to the montmorillonite content in MX-80 bentonite (75 weight %), another inconsistency would be introduced, since this procedure would neglect the

contribution of hydroxyl surface sites by minor oxides (25 weight % of the bentonite consist almost exclusively of quartz and feldspar, see MÜLLER-VONMOOS and KAHR, 1983). Thus, for our model we preferred to avoid any scaling of surface site concentrations. The error introduced in this way is certainly small compared to other critical parameter uncertainties.

Table 3.1: Overview of model parameters, properties of MX-80 bentonite and Opalinus Clay water composition used for the derivation of the reference bentonite porewater.

	Value	**Reference**
solid:water (S/W) ratio [kg L^{-1}]	4.5032	[1]
Temperature [^{0}C]	25	[1]
log pCO_2 [bar]	-2.2	[2]
surface complexation		
BET surface area [m^2 kg^{-1}]	31300	[3]
surface site concentrations:		
$\{=X_1OH\}_{tot}$ [eq. kg^{-1}]	0.042	[4]
$\{=X_2OH\}_{tot}$ [eq. kg^{-1}]	0.040	[4]
surface complexation constants:		
log $K_{int}(=X_1OH_2^+)$	4.5	[4]
log $K_{int}(=X_1O^-)$	-7.9	[4]
log $K_{int}(=X_2OH_2^+)$	6.0	[4]
log $K_{int}(=X_2O^-)$	-10.5	[4]
initial speciation of surface sites	100 % $=XOH^0$	assumed
ion exchange		
CEC [eq kg^{-1}]	0.787	[5]
initial occupancies (equiv. fraction):		
Na^+	0.848	[5]
Ca^{2+}	0.084	[5]
Mg^{2+}	0.051	[5]
K^+	0.017	[5]
H^+	0	[5]
Sr^{2+}	0	[5]
selectivity coefficients:		
${}^{Ca}_{Na}K_c$	2.6	[5]
${}^{K}_{Na}K_c$	4.0	[5]
${}^{Mg}_{Na}K_c$	2.2	[5]
${}^{Sr}_{Na}K_c$	2.6	[5]
${}^{H}_{Na}K_c$	1.0	[5]

	Value	Reference
saturated solids	**log K_s^0**	
quartz, SiO_2 (s) + 2 H_2O = H_4SiO_4	-3.98	[7]
calcite, $CaCO_3(s) = Ca^{2+} + CO_3^{2-}$	-8.48	[6]
kaolinite, $Al_2Si_2O_5(OH)_4$ (s) + 6H^+ = 2 Al^{3+} + 2 H_4SiO_4 + H_2O	+7.44	[7]
gypsum, $CaSO_4$. 2 $H_2O(s)$ = 2 H_2O +Ca^{2+} + SO_4^{2-}	-4.58	[6]
soluble solids	inventory [mol kg^{-1}]	
halite	1.35 x 10^{-3}	[5]
reacting water (Opalinus Clay)		
pH	7.24	[2]
Ionic strength [eq. L^{-1}]	0.228	[2]
Solution composition:	[mol L^{-1}]	
Na	0.169	[2]
K	5.65 x 10^{-3}	[2]
Mg	7.48 x 10^{-3}	[2]
Ca	1.05 x 10^{-2}	[2]
Sr	3.04 x 10^{-4}	[2]
Carbonate	2.70 x 10^{-3}	[2]
Sulphate	2.40 x 10^{-2}	[2]
Cl	0.160	[2]

References: [1] based on data given in JOHNSON and SCHNEIDER (2000); [2] PEARSON (2002); [3] BRADBURY and BAEYENS (1998); [4] BRADBURY and BAEYENS (1997); [5] BRADBURY and BAEYENS (2002a); [6] PEARSON and BERNER (1991); [7] PEARSON et al. (1992).

Cation exchange properties are taken from recent Ni-ethylendiamine extraction data (BRADBURY and BAEYENS, 2002a). The derived cation occupancies and cation exchange capacities (CEC) compare well with the determinations of MÜLLER-VONMOOS and KAHR (1983), which were made on the same material but with a different technique (exchange with ammonium acetate). From fractional occupancies and aqueous concentrations, BRADBURY and BAEYENS (2002a) derived the selectivity coefficients for K-Na, Ca-Na and Mg-Na listed in Table 3.1. The same authors also give estimates of selectivity coefficients for Sr-Na and H-Na, which we also adopted. For modelling purposes, the selectivity coefficients K_c were transformed into exchange constants, K_{ex} , normalised to solution volume, yielding K_{ex}(Ca-Na) = 0.37, K_{ex}(K-Na) = 4.0, K_{ex}(Mg-Na) = 0.31, K_{ex}(Sr-Na) = 0.37, and K_{ex}(H-Na) = 1.0 (see Appendix D for details on the transformation).

The selection of reactive solids relies on mineralogical analyses of the MX-80 bentonite (MÜLLER-VONMOOS and KAHR, 1983) and on recent aqueous extraction data (BRADBURY and BAEYENS, 2002a). The mineralogical analyses revealed the presence of a number of accessory minerals (quartz, feldspar, calcite, siderite, micas, chlorite, zircon, pyrite, kaolinite). Only calcite, kaolinite and quartz were assumed to be in saturation equilibrium

(BRADBURY and BAEYENS, 1995; WIELAND et al., 1994). Since kaolinite and quartz saturation were assumed, the Si and Al concentrations are fixed by these two equilibria. The aqueous extracts revealed the presence of small amounts of sulphate and chloride in the MX-80 samples, which were interpreted in terms of gypsum and halite dissolution (BRADBURY and BAEYENS, 2001; WANNER et al., 1992). These two minerals have been modelled as mass limited solids, i.e. dissolution was allowed in the model calculations up to the consumption of their inventories in MX-80. For gypsum, the inventory of 23.5 mmol kg^{-1} (BRADBURY and BAEYENS, 2001) is sufficient to saturate the porewater at S/W = 4.5 kg L^{-1}. Gypsum appears therefore as saturated solid in Table 3.1. On the contrary, the amount of NaCl inferred from the aqueous extracts is far too low to reach halite saturation, even at such high S/W ratios. The remaining minerals are either inert at the low temperatures involved (e.g. micas, zircon) or are predicted to dissolve under the redox conditions assumed (e.g. siderite).

3.3 Model testing: comparison with experimental data

3.3.1 Introductory remarks

A major aim was to test our geochemical model against suitable experimental data before applying it to derive the reference bentonite porewater. We decided to base our testing on the recent experimental data of MUURINEN and LEHIKOINEN (1999), who studied in detail the long-term interaction of MX-80 bentonite with both diluted and saline waters. This selection was made on the base of the long interaction times and high S/W ratios imposed in these experiments.

3.3.2 Setup of the Finnish experiments

The selected experiments were carried out in a closed reactor cell filled with water-saturated bentonite at the desired S/W ratio. At end-reaction time, a small volume of porewater (0.5 -1.5 mL) was squeezed out through a sinter filter by means of a hydraulic piston. For S/W ratios above ~ 0.1 kg/L, the concentrations of dissolved species depend on the extraction technique. The total dissolved salt content of the extracted porewater was found to decrease with increasing squeezing pressure. MUURINEN and LEHIKOINEN (1999) interpreted these results as an indication of ion exclusion. As the squeezing pressure increases, the separation between adjoining clay particles would decrease to the point where the diffuse double layers of adjacent particles begin to interact, hindering the movement of charged species.

In the attempt to obtain more representative data, MUURINEN and LEHIKOINEN (1999) devised an alternative set-up, in which the cell containing the saturated bentonite was put in contact with an "external water" reservoir through a steel sinter of 2 μm pore size. After sufficient reaction time (1-2 years), an overall chemical equilibrium, more representative of the pore solution inside the bentonite sample, was established via diffusion. These external solutions were up to five times more concentrated than the squeezed porewaters, suggesting that ion exclusion effects were negligible in this type of test.

3.3.3 Selection of experimental data and modelling parameters

For our model test, we selected only data obtained from this second type of experiments. The results of 16 experiments and the composition of the initial water are shown in Table 3.2. The initial and final exchanged ion populations were also determined for each experiment (see Table A-1, Appendix A).

The parameters used for the modelling of these data are presented in Table 3.3. The calculations for "Model 1" are based on the surface complexation and cation exchange constants of WIELAND et al. (1994). "Model 2" refers to calculations performed using the surface complexation constants and selectivity coefficients of BRADBURY and BAEYENS (1997). These are identical to those selected to model the reference porewater (reported in Table 3.1).

Table 3.2: Equilibration experiments of MUURINEN and LEHIKOINEN (1999). Other experimental data of that study (e.g., squeezing experiments, "dynamic" experiments) were not used in this work.

Exp. run	**S/W** Mg/m^3	**pH**	**Na** mmol/L	**K** mmol/L	**Ca** mmol/L	**Mg** mmol/L	**Cl** mmol/L	**SO_4** mmol/L	**CO_3** mmol/L
	bentonite equilibrated with fresh water								
01	0.5	8.8	74	0.61	0.95	0.49	8.3	33	8.6
02	0.015	9.0	5.0	0.13	0.18	0.16	1.7	0.72	2.4
03	1.5	8.4	247	1.71	9.06	4.0	5.7	129	3.6
04	0.015	9.2	4.5	0.17	0.13	0.11	1.8	0.73	1.9
05	1.5	8.6	189	1.25	4.69	2.4	11.7	98	7.0
06	0.5	8.7	56	0.41	0.80	0.45	6.1	26	5.3
07	0.1	8.6	13	0.24	0.36	0.28	2.2	4.4	3.3
08	0.015	8.8	4.2	0.14	0.15	0.16	1.7	0.7	2.0
09	0.015	8.7	3.6	0.11	0.20	0.19	1.7	0.47	1.6
	bentonite equilibrated with saline water								
10	1.5	8.1	509	2.9	39	14.0	466	33	1.4
11	0.015	7.7	181	0.5	82	2.1	336		0.3
12	1.5	8.1	522	2.4	39	13.0	498	34	2.7
13	0.5	8.0	349	1.5	47	9.4	398	14	2.1
14	0.1	7.9	249	1.0	79	5.3	398	3.0	1.2
15	0.015	7.7	207	0.5	95	2.4	390		0.3
16	0.015	7.5	202	0.4	95	2.4	381		0.2
	initial waters								
fresh		9.1	2.3	0.10	0.46	0.19	1.5	0.10	1.80
saline		8.2	209	0.5	100	2.3	417	0.0044	0.0035

Table 3.3: Parameters used to model the experimental data of MUURINEN and LEHIKOINEN (1999).

miscellaneous parameters	Model 1 & Model 2	
solid:water (S/W) ratio [kg L^{-1}]	1.5	
Temperature [^{0}C]	25	
log pCO_2 [bar]	-3.5	
surface complexation	Model 1	Model 2
BET surface area [m^2 kg^{-1}]	31500	31500
surface site concentrations:		
$\{=X_1OH\}_{tot}$ [eq. kg^{-1}]	0.0284	0.042
$\{=X_2OH\}_{tot}$ [eq. kg^{-1}]	-	0.040
surface complexation constants:		
log $K_{int}(=X_1OH_2^+)$	5.4	4.5
log $K_{int}(=X_1O^-)$	-6.7	-7.9
log $K_{int}(=X_2OH_2^+)$	-	6.0
log $K_{int}(=X_2O^-)$	-	-10.5
initial speciation of surface sites:	100 % $=XOH^0$	100 % $=XOH^0$
ion exchange	Model 1 & Model 2	
CEC [eq. kg^{-1}]	0.750*	
initial occupancies (equiv. fraction):		
Na^+	0.808	
Ca^{2+}	0.128	
Mg^{2+}	0.055	
K^+	0.009	
H^+	0	
selectivity coefficients:	Model 1	Model 2
${}^{Ca}_{Na}K_c$	1.62	2.6
${}^{K}_{Na}K_c$	1.82	4.0
${}^{Mg}_{Na}K_c$	1.35	2.2
${}^{H}_{Na}K_c$	3.0	1.0
saturated solids	Model 1 & Model 2 (log K^0_s)	
quartz SiO_2 (s) + 2 H_2O = H_4SiO_4	-3.98	
calcite $CaCO_3$(s) = Ca^{2+} + CO_3^{2-}	-8.48	
kaolinite $Al_2Si_2O_5(OH)_4$ (s) + 6H^+ = 2Al^{3+} + 2H_4SiO_4 + H_2O	+7.44	
gypsum $CaSO_4$. 2H_2O(s) = Ca^{2+} + SO_4^{2-}	-4.58	

* The CEC of 0.750 eq. g^{-1} was selected before the new determination (0.787 eq. g^{-1}) of BRADBURY and BAEYENS (2002a) was available and corresponds approximately to the value given by MÜLLER-VONMOOS and KAHR (1983).

3.3.4 Modelling results

The solution compositions reported in Table 3.2 from MUURINEN and LEHIKOINEN (1999) were evaluated by means of speciation calculations. These revealed, to our surprise, considerable oversaturation with respect to calcite in both initial and final solutions. As discussed in Appendix A, our calculations indicate loss of CO_2 after preparation of the reacting solutions, thereby leading to calcite oversaturation via pH increase. The solutions were however apparently stable, as no precipitate was observed at any time during the experiments (MUURINEN, pers. comm.). For our modelling, we therefore assumed a constant calcite saturation index of 0.9 and pCO_2 of $10^{-3.2}$ bar, as indicated by the results of our calculations. The precise input data for the two models considered are listed in Table 3.3.

Most results of both "Model 1" and "Model 2" are in satisfactory agreement with the experimental data over the entire range of S/W ratios. This is illustrated in Figure 3.2, which shows a comparison of the modelled Na, Ca, Mg, K, Cl, SO_4, CO_3 concentrations and pH with experimental data for the "fresh water" experiments across the whole S/W range. In general, deviations from the experimental values are less than a factor of three. Note that predicted pH-values agree within 0.2 units with the analytical values. In the case of the experiments carried out with "saline" solutions (Table 3.2) both models show agreement within a factor of two (data not shown). The agreement is remarkable given the rather large scatter in the experimental data and the mentioned experimental problems (e.g. leakage of CO_2).

The modelling of the experiments carried out at S/W= 1.5 kg/L (exp. runs 03 and 05 in Table 3.2) will be commented in some detail. These results are presented in Figure 3.3 and Table 3.4, where four columns are distinguished. Column one specifies the initial state of the system, i.e. the composition of the reacting water and the initial occupancies of exchanged cations, as given in the original reference. Column two gives the analytical results after reaction with the bentonite, while columns three and four report the results of our two models.

A detailed examination of the results of our chemical calculations indicates that the porewater composition is controlled by a few key reactions. These are:

a) exchange of Ca for Na;

b) deprotonation of surface hydroxyl groups;

c) loss of carbon dioxide.

The deprotonation of surface hydroxyl groups is a direct consequence of the high pH (9.1) of the initial solution and of the model assumption that all groups in the initial surface are present as uncharged $=XOH^o$ species. This process is partly counterbalanced by dissolution of calcite and CO_2 loss. A net acidification of the solution results, since the amount of protons released by the surface hydroxyl groups exceeds the amount consumed through calcite dissolution and CO_2 escape. Both models predict a pH-decrease by almost one unit (from 9.1 to 8.2-8.3), which is only slightly below the analytical value of 8.4.

Finally, we note that the results obtained using the two alternative sets of constants for surface complexation and cation exchange reactions are very similar, except for the large difference in the calculated loadings of exchanged protons. The latter discrepancy derives from the largely different H-Na exchange constants assumed in either model. In the pH region of interest, however, the absolute amounts of exchanged protons are negligible and have no influence on porewater composition.

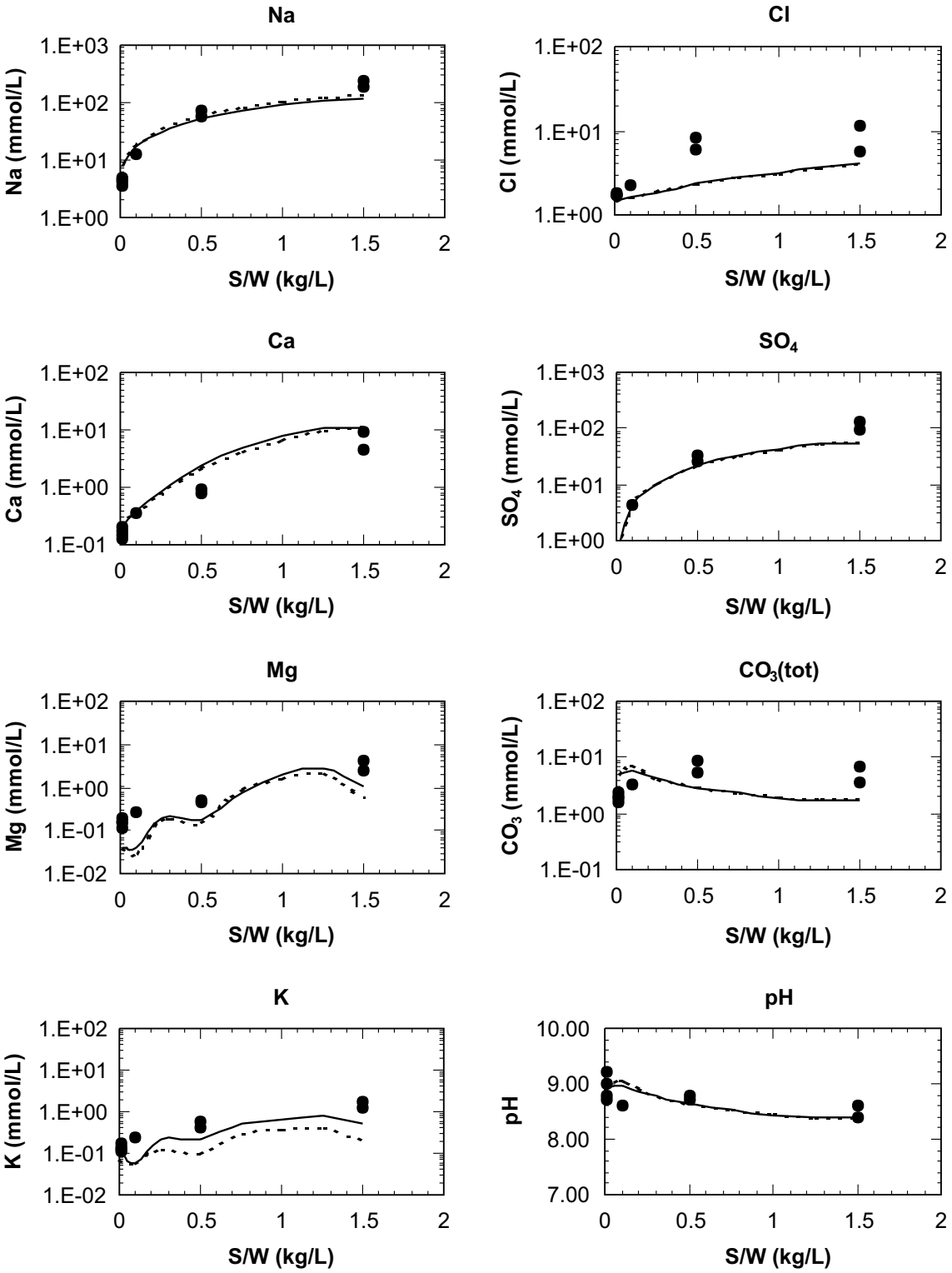

Figure 3.2: Comparison between experimental data from the "fresh water" experiments of MUURINEN and LEHIKOINEN (1999) (dots), Model 1 (solid line) and Model 2 (dashed line).

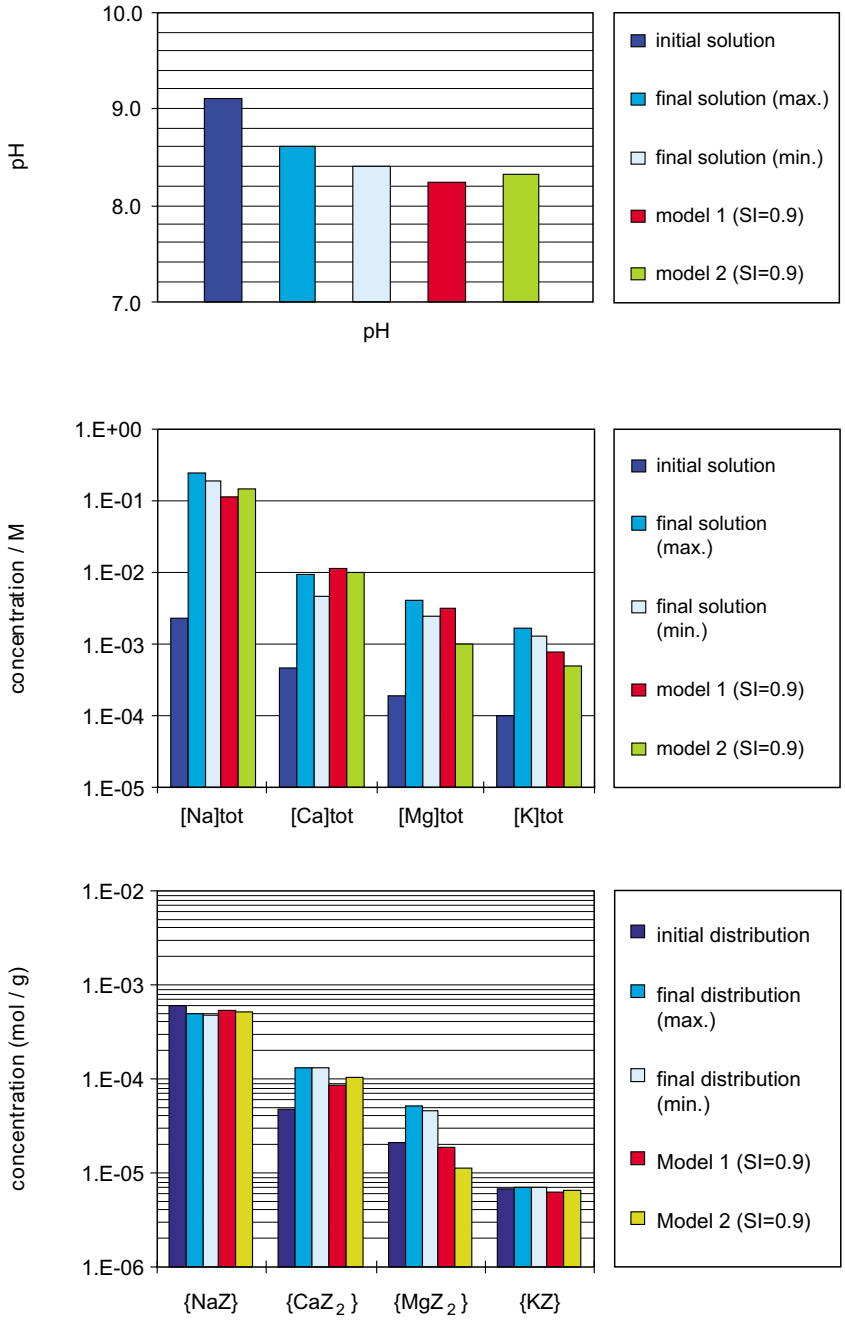

Figure 3.3: Comparison of model calculations for the equilibrated MX80-bentonite porewater at S/W=1.5 kg/L with the corresponding analytical data of MUURINEN and LEHIKOINEN (1999). Dark blue bars denote solution composition and exchanged ion populations before reaction. Light blue bars show the maximum and minimum values after reaction.

Table 3.4: Comparison of analytical data and model calculations for selected water-bentonite interaction experiments conducted at S/W = 1.5 kg L^{-1} from MUURINEN and LEHIKOINEN (1999).

	Initial conditions	**Experimental data**	**Model 1**	**Model 2**
solution [mmol L^{-1}]	Muurinen and Lehikoinen (1999) Table 1, p.7	Muurinen and Lehikoinen, (1999) App. A1, p.35	Wieland et al. (1994)	Bradbury and Baeyens (1995)
pH	9.1	8.4*	8.2	8.3
Ionic strength / M	0.004	0.33	0.16	0.20
SI calcite	0.9	0.9	0.9	0.9
log pCO_2 /bar	- 4.1	-3.2	-3.2	-3.2
Na	2.26	247	117	146
Ca	0.464	9.06	11.2	9.92
Mg	0.19	4.0	3.12	0.99
K	0.10	1.71	0.78	0.48
Cl	1.48	5.7	5.70	5.70
SO_4	0.10	129	53.8	74.8
CO_3	1.8	3.6	2.51	2.95
exchanged cations [mmol kg^{-1}]	Muurinen and Lehikoinen (1999) Table 2, p.10	Muurinen and Lehikoinen (1999) App. A4, p.38		
{NaZ}	606	486	532	513
$\{MgZ_2\}$	20.6	22.5	18.7	11.4
$\{CaZ_2\}$	48.0	65.5	87.0	104
{KZ}	6.75	7.0	6.3	6.5
{HZ}	n.d.	n.d.	0.036	2.5E-05
solids & gases [mmol L^{-1}]				
CO_2(g) escaped			14.8	40.0
calcite dissolved			-15.5	-41.2
gypsum dissolved			-53.7	-74.7
surface complexes [mmol L^{-1}]				
$[=X_1OH]$			11.7	17.5
$[=X_1OH_2^+]$			0.2	0.003
$[=X_1O^-]$			30.7	45.5
$[=X_1O]_{tot}$			42.6	63.0
$[=X_2OH_2^+]$				0.1
$[=X_2OH]$				24.0
$[=X_2O^-]$				0.2
$[=X_2OMg^+]$				13.1
$[=X_2OCa^+]$				22.6
$[=X_2OH]_{tot}$				60.0

* in order to fit the results of the chemical model to the measured pH of 8.4, a small amount of sulphuric acid must be added, leading to a sulphate concentration slightly larger than indicated by the analysis (133 instead of 129 mmol/L). This modification is well within the analytical uncertainty for sulphate.

3.4 Calculation of bentonite porewater under repository conditions

In spite of the uncertainties concerning the equilibrium state of the solutions (CO_2 loss, calcite oversaturation), the data of MUURINEN and LEHIKOINEN (1999) could be reproduced satisfactorily by our chemical model with either set of sorption constants ("Model 1" and "Model 2"). Following this successful test, the model has been judged suitable to define reference bentonite porewater compositions for the high-level waste repository planned in the Opalinus Clay formation.

The basic assumptions implied in our water-bentonite interaction model are summarised again in Table 3.5. The impact of these assumptions has been tested in a sensitivity analysis (see section 3.5), showing that some of these assumptions influence critically the porewater chemistry, whereas others have only small effects on the final results.

Table 3.5: Basic assumptions made in the geochemical model used for the derivation of the bentonite porewater.

Model assumption	**Parameters affected**	**Basis for the choice**
The bulk of the water saturating the bentonite is available to dissolved species. No distinction between interlayer and external water is made.	Porosity, ε =0.38 Solid/water ratio, S/W = 4.5 kg/L	In compacted bentonite, clay particle separations are comparable to the width of structural interlayer of expanded montmorillonite (Appendix B)
System open to gas exchange	pCO_2 fixed at $10^{-2.2}$ bar	PEARSON (2002) Diffusive processes in bentonite are fast relative to timescales of interest
Protonation of surface hydroxyl groups is independent of surface charge ("non-electrostatic" model)	fixed values for: log K ($=X_1OH_2^+$) log K ($=X_1O^-$) log K ($=X_2OH_2^+$) log K ($=X_2O^-$)	BRADBURY and BAEYENS (1997) Modelling of detailed experimental data indicates that an electrostatic term is not required
The initial distribution of surface hydroxyl groups is 100 % $=XOH^0$	$[=X_1OH^0] + [=X_2OH^0] = [=XO]_{tot}$ $[=X_1OH_2^+] = [=X_2OH_2^+] = 0$ $[=X_1O^-] = [=X_2O^-] = 0$	Arbitrary choice: the initial state of the surface is not known
Temperature fixed at 25 °C	all equilibrium constants	All thermodynamic data refer to 25 °C. A consistent extrapolation of all constants to higher temperatures is not possible

The model for the reference bentonite porewater is essentially identical to that applied to describe the experiments of MUURINEN and LEHIKOINEN (1999). However, different boundary conditions are imposed under repository conditions:

a) A higher S/W ratio (4.5 kg/L) applies in the repository. This corresponds to an increase in compaction by a factor of three.

b) Different CO_2 partial pressures, with pCO_2 fixed at $10^{-2.2}$ bar in the reference case and $10^{-3.5}$ / $10^{-1.5}$ bar as bounding values (PEARSON, 2002).

For the calculation of the bentonite porewater we rely on the surface complexation and ion exchange data specified for "Model 2", which are based on the extensive characterisation and modelling work of BRADBURY and BAEYENS (1997; 1998; 2002) for MX-80 bentonite. This model has been preferred because of its internal consistency, as it predicts, using a few fixed thermodynamic parameters, a large number of sorption data over a wide range of pH and ionic strengths. An important feature of this surface complexation model is that no electrostatic potential correction of the surface complexation constants is applied. These have thus fixed values, independent of the charge on the surface.

The model assumes fixed pCO_2 conditions imposed by the surrounding host rock. This assumption was selected on the basis of the long timescales (≈ 10'000 - 100'000 years) that are of interest for many phenomena in performance assessment[1]. Simple analytical transport calculations (SMITH, written communication) suggest that diffusion of non-sorbing, uncharged solutes through the bentonite backfill is fast relative to these timescales.

Table 3.6 reports the composition of the bentonite porewater calculated for repository conditions from the input data specified in Table 3.1, resulting from the reaction of MX-80 bentonite with the Opalinus Clay reference water. Predicted changes in pH, major dissolved species and exchanged ion concentrations are shown as bar diagrams in Figure 3.4.

[1] 10'000 years is the assumed time of waste canister breaching in the Swiss SF/HLW repository.

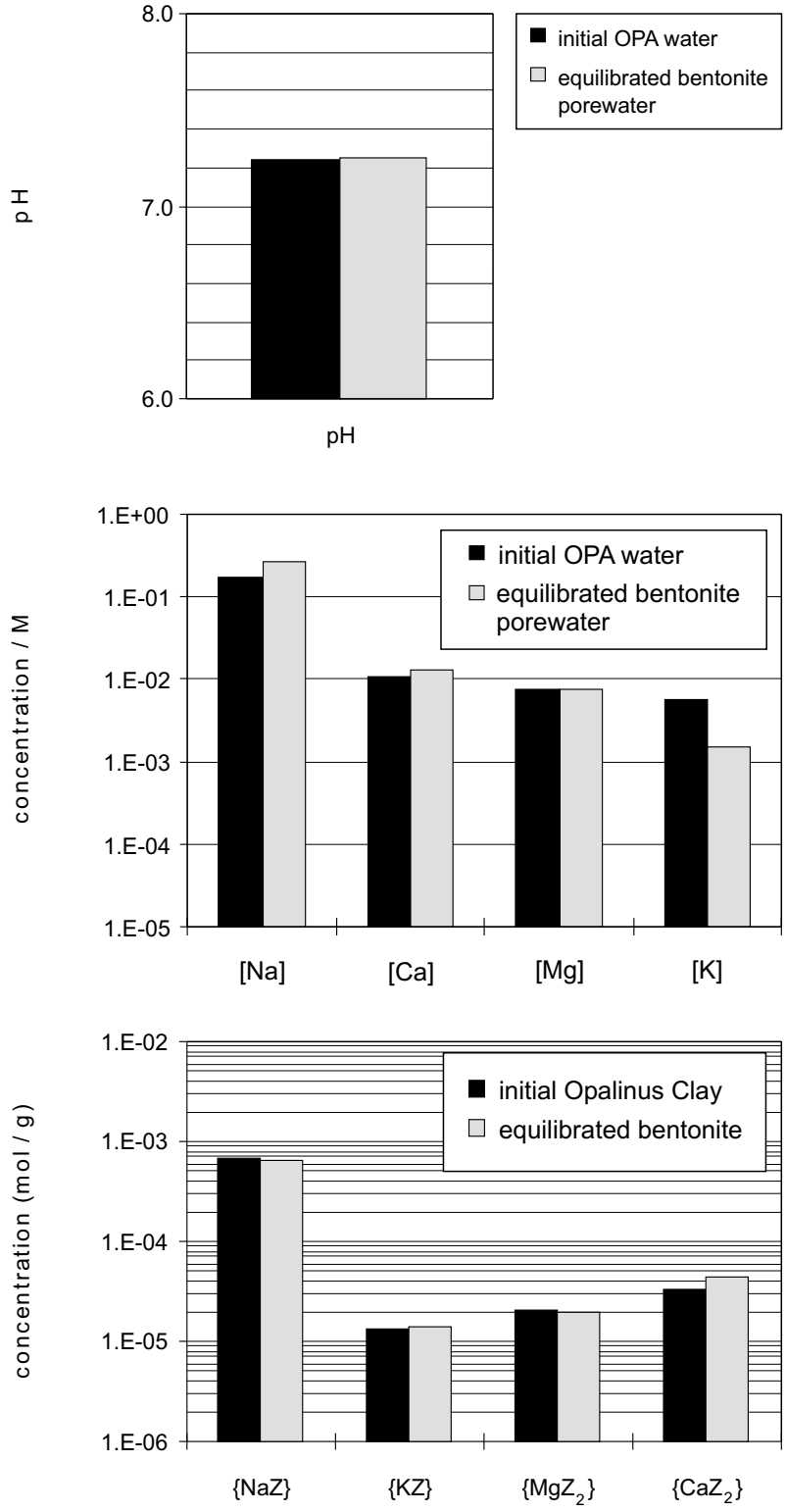

Figure 3.4: Bar chart representation of the results obtained for the reference bentonite porewater calculations. Equilibrated porewater and exchanged ion compositions are compared to the initial reference Opalinus Clay water composition and to the exchanged ion populations in the unreacted MX-80 bentonite, respectively.

Table 3.6: Composition of Opalinus Clay reference water (D-OPA) and bentonite porewater (D-RBPW) calculated from the reaction between Opalinus Clay water and MX-80 bentonite, using the input data specified in Table 3.1. The initial and final distributions of exchanged cations and surface hydroxyl species are also given.

	D-OPA (input water)	**D-RBPW (reacted water)**
log pCO_2 [bar]	-2.2	-2.2
pH	7.24	7.25
Ionic strength [eq./L]	0.23	0.32
dissolved species [mol/L]		
CO_3	2.70×10^{-3}	2.83×10^{-3}
Na	1.69×10^{-1}	2.74×10^{-1}
Ca	1.05×10^{-2}	1.32×10^{-2}
Sr	3.04×10^{-4}	1.90×10^{-5}
Mg	7.48×10^{-3}	7.64×10^{-3}
K	5.65×10^{-3}	1.55×10^{-3}
Al	n.d.	1.92×10^{-8}
SO_4	2.40×10^{-2}	6.16×10^{-2}
Cl	1.60×10^{-1}	1.66×10^{-1}
Si	n.d.	1.80×10^{-4}
exchanged cations [mol/g]	**MX-80 (before reaction)**	**MX-80 (post reaction)**
$\{Na^+\}$	6.67×10^{-4}	6.45×10^{-4}
$\{Ca^{2+}\}$	3.31×10^{-5}	4.36×10^{-5}
$\{Mg^{2+}\}$	2.00×10^{-5}	2.00×10^{-5}
$\{K^+\}$	1.34×10^{-5}	1.43×10^{-5}
surface species [mol/L]		
=XOH	3.69×10^{-1}	3.25×10^{-1}
$=XOH_2^+$	-	9.84×10^{-3}
$=XO^-$	-	3.47×10^{-2}
=XO(total)	-	3.69×10^{-1}
surface charge [mol/L]	-	-2.48×10^{-2}

The results indicate that pH and porewater composition are largely controlled by the same reactions identified in the modelling of the Finnish data, i.e. the displacement of exchanged Na^+ by Ca^{2+}, deprotonation of surface hydroxyls, dissolution of Ca minerals and CO_2 loss. The Na-Ca exchange reaction is the driving force for the partial dissolution of gypsum and calcite. Due to dissolution of gypsum, NaCl and calcite, and because of the high S/W ratio, a significant increase in ionic strength (from 0.23 to 0.32 mol/L) is predicted. Conversely, a slight increase in total carbonate concentration results from calcite dissolution, which is only partially counterbalanced by CO_2 loss.

Deprotonation of the surface hydroxyl groups leads to a negative surface charge (-24 μC m^{-2}). Hence, a formal positive charge (2.48 x 10^{-2} eq/L) results in the aqueous phase. This excess charge is due to counter ions concentrated in the diffuse double layer (which can be regarded as loosely adsorbed on the external clay surfaces). The MINSORB code makes no explicit account of anion exclusion in the double layer and calculates only a bulk aqueous phase, in which the contributions of double layer and charge-balanced external water are averaged. That is, no distinction is made between the double layer region (where anions are excluded) and the rest of the (electrically balanced) external porewater.

It is still an open question whether such distinctions can be made in compacted bentonites, where clay particle separations drop to a few nanometres. Under such conditions, the diffuse double layers of adjoining clay particles will tend to overlap, and the existence of an electrically neutral solution zone, through which charged species can diffuse freely, becomes questionable. Therefore, we prefer to regard the resulting positively charged aqueous phase as an intrinsic, inseparable part of the surface complexation model[2]. To assess the potential impact of anion exclusion on porewater composition a refined model, explicitly accounting for double layer effects, was developed. The results indicate that ion exclusion effects are of minor importance. These issues are treated in detail in chapter 3.5.5, Appendix B and Appendix E.

3.5 Sensitivity analysis

3.5.1 Preliminary remarks

A sensitivity analysis was carried out to determine quantitatively the influence of parameter uncertainties and assumptions on the calculated porewater composition. We tried to identify critical variables with the help of simple chemical reasoning, thereby avoiding time-consuming parameter variations. Our analysis of the bentonite system revealed that the porewater chemistry is largely controlled by a few critical parameters. In this section we deal only with the initial composition of the bentonite porewater. Effects related to the temporal evolution of the porewater are discussed in chapter 4.

3.5.2 Effect of initial site distribution

One of the basic implicit assumptions in our model concerns the initial distribution of surface hydroxyl species. At the start of the reaction all hydroxyl surface sites are assumed to be uncharged (i.e. $[=XOH]_{tot} = [=XOH]$; $[XO^-] = [XOH_2^+] = 0$). This assumption is arbitrary and dictated only by convenience. The initial state of the =XO sites in the bentonite sealing the repository tunnels will depend on the geological history of the bentonite formation and on the subsequent industrial processing. Rather than trying to reconstruct these complex processes, in this section we explore in detail the consequences of assuming different initial distributions of the surface hydroxyl species and show that the final equilibrium distribution is almost insensitive to this parameter. From this insight, it is then concluded that a precise knowledge of the initial surface speciation is not critical for our modelling.

Let us assume that the initial site distribution is characterised by a large excess of deprotonated sites (i.e. $[XO^-] > [XOH_2^+]$). The surface would then act as a base and consume protons instead of releasing them as in the previous calculation. In order to do realistic calculations with this alternative assumption, one must however start with an electrically neutral bulk system. This

[2] Note that "charged solutions" are generated also when modelling dilute clay suspensions. In this case, however, the S/W ratios are so low, that the net charge concentration in the formal aqueous phase becomes negligible.

means that the assumed excess of deprotonated sites must be balanced by an equivalent amount of adsorbed cations. In principle, one would need to know the amounts of such cations and the corresponding sorption constants, but such detailed information is in general not available.

To evaluate this effect we assume Na^+ to be the main charge balancing cation and regard it as a loosely adsorbed (outer sphere) complex sticking on the external surface of the initial dry bentonite. This sodium is regarded as completely soluble upon contact with water and can thus be readily exchanged with interlayer cations when the clay is wetted. We thus simulate a variable excess of deprotonated sites by "titrating" the reference bentonite porewater with a fictitious surface complex $=XO^-$ -- Na^+, which dissociates completely in water.

The results of such titrations are shown in Figure 3.5, where the abscissa indicates the initial net excess of deprotonated surface hydroxyl species (as a fraction of the total site concentration[3]), and the ordinate indicates the distribution of surface hydroxyl species resulting at equilibrium. Our calculations[4] indicate that the equilibrium distribution of surface hydroxyl species is almost insensitive to the initial distribution. Even if all edge sites were initially protonated (100 % as $=XOH_2^+$), deprotonated $=XO^-$ sites would still be in excess of $=XOH_2^+$ at equilibrium. The net difference of this excess for the two extreme initial conditions considered (i.e. assuming 100 % $=XOH_2^+$ or 100 % $=XO^-$ at the start of the reaction) is only ~0.015 eq./L or about 4 % of the total site inventory.

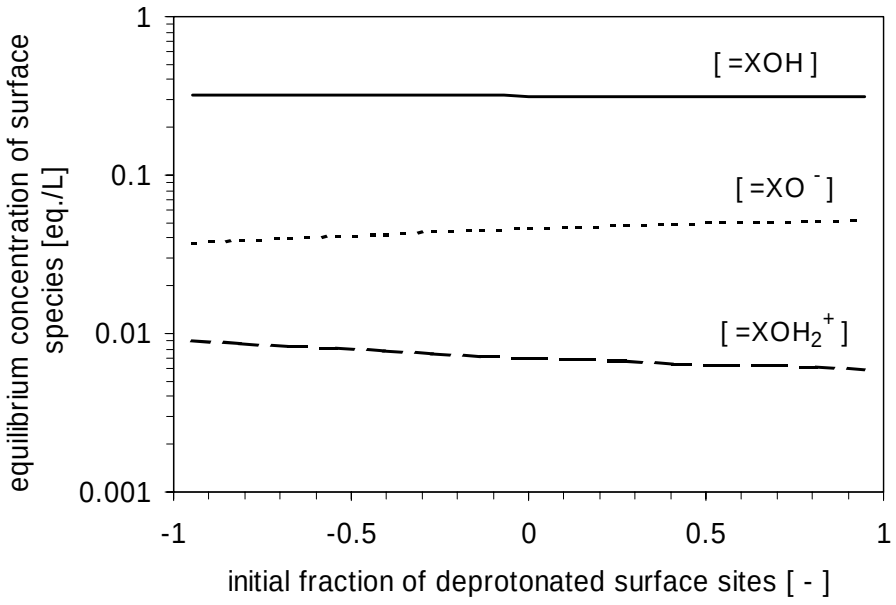

Figure 3.5: Effect of the initial distribution of surface hydroxyl sites on their equilibrium distribution for bentonite porewater equilibrated with MX-80.

[3] This quantity is equal to 1 when all sites are deprotonated (100 % $=XO^-$), is equal to 0 for 100 % =XOH and is equal to -1 when all sites are protonated (100 % $=XOH_2^+$).

[4] These calculations were performed before the reference Opalinus Clay water became available, using a preliminary composition at $pCO_2 = 10^{-3.5}$ bar. Although slightly more alkaline bentonite pore waters are obtained in this way, the following arguments also fully apply to the final reference bentonite pore water.

3.5.3 Buffering mechanism

This result and the relatively small pH variation (7.6 and 8.0 with the two extreme initial conditions, see Figure 3.6) indicate that the system is well buffered. The buffering effect is due to neutralisation of the acidity produced by surface hydroxyl deprotonation through calcite dissolution and CO_2 escape (or the reverse reaction if protonation of the surface hydroxyl groups occurs):

$$2 \equiv XOH^0 \leftrightarrow 2 \equiv XO^- + 2\ H^+$$
$$CaCO_3(s) + 2\ H^+ \leftrightarrow Ca^{2+} + CO_2(g) + H_2O$$

The net neutralisation reaction is:

$$CaCO_3(s) + 2 \equiv XOH^o \leftrightarrow Ca^{2+} + CO_2(g) + 2 \equiv XO^- + H_2O.$$

This mechanism is evidenced by the correspondence of the computed mass transfers (Figure 3.6): as required by the stoichiometry of the reactions above, the moles of CO_2 lost (or absorbed) match the moles of calcite dissolved (or precipitated) and the amounts of deprotonated (or protonated) surface hydroxyls are twice the moles of calcite dissolved (or precipitated). The stability of this buffering mechanism depends of course on the availability of calcite. Due to the very high S/W ratio, the amount of calcite dissolved to reach equilibrium is very small and less than the initial mineral inventory. In chapter 4, we show that the calcite inventory will not be dissolved further in the course of the predicted porewater evolution. Therefore, the buffering effect is expected to persist in the course of repository evolution.

The neutralisation reaction has a side effect on the final exchanged ion distribution, as depicted in Figure 3.7. For a fully deprotonated initial surface hydroxyl population, the neutralisation reaction would proceed to the left, thus removing Ca ions from solution. As a result, the final ratio of exchanged Ca to Na would decrease. Starting with a fully protonated surface would have the opposite effect due to enhanced dissolution of calcite. However, these effects are not very significant and would not change the main system characteristics.

In conclusion, these calculations show that in compacted bentonite systems open to gas exchange and in the presence of calcite the initial distribution of surface hydroxyl species has only a minor influence on the final equilibrium state. This conclusion is important, since it allows us to infer that the uncertainty about the initial speciation of the hydroxyl surface has only a limited influence on composition and pH of the bentonite porewater.

It is however important to realise that in systems closed to gas exchange and in the absence of reactive carbonates, the buffering mechanisms described above would not operate. In such systems, the initial distribution of surface hydroxyl species would have an important effect on the equilibrium pH of the porewater. In our opinion, it is unlikely that the bentonite backfill will be closed to carbon dioxide exchange with the surrounding under repository conditions. Dissolved gas molecules are uncharged, thus CO_2 diffusion into or out of the bentonite should not be hindered through surface electrostatic effects.

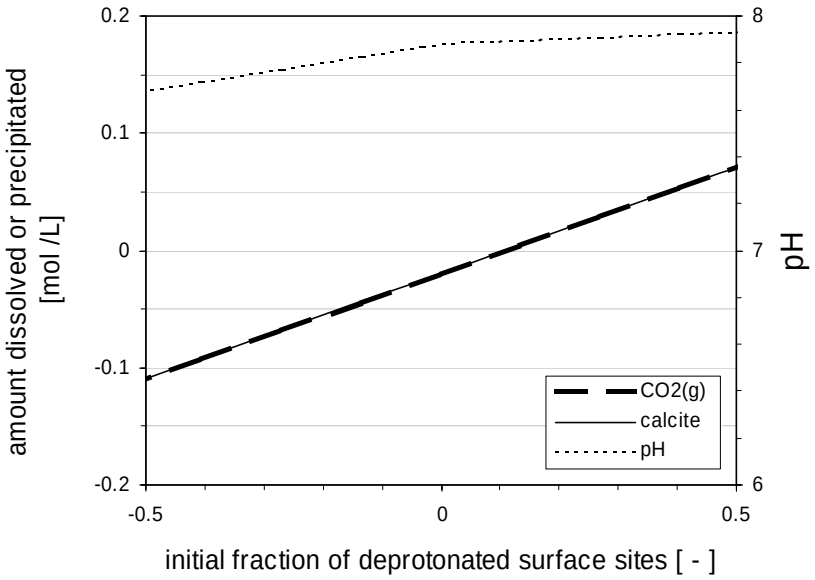

Figure 3.6: Calculated pH and mass transfers for calcite dissolution (-) / precipitation (+) and CO_2 loss (-) / uptake (+) as a function of the initial distribution of hydroxyl surface sites on MX-80 bentonite.

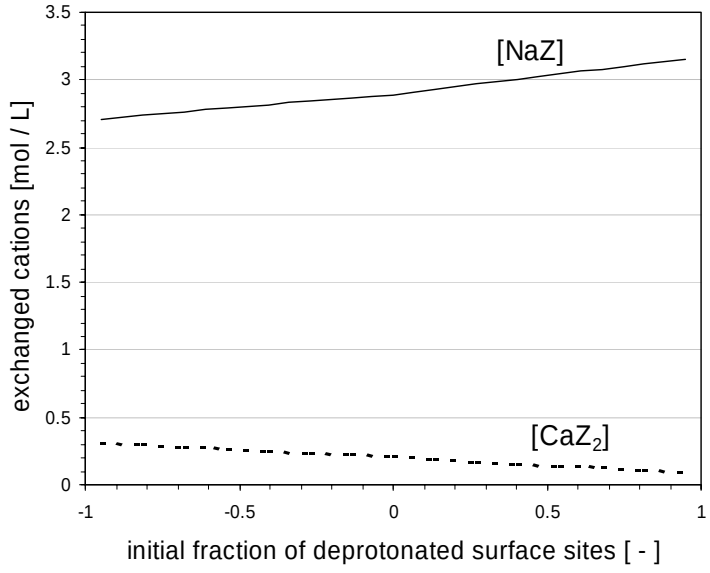

Figure 3.7: Influence of the initial distribution of hydroxyl surface sites on the final distribution of exchanged Ca and Na.

3.5.4 Effect of the carbonate system and minor minerals.

The preceding calculations reveal the key role of carbonate species in buffering pH and porewater composition. However, it is presently difficult to specify reliable CO_2 partial pressures in the Opalinus Clay formation. According to current understanding, the uncertainty for this parameter is about two orders of magnitude. Thus, a variation between $10^{-3.5}$ and $10^{-1.5}$ bar has to be considered, in agreement with the boundaries proposed by PEARSON (2002).

The pH of a solution in equilibrium with calcite at constant CO_2 partial pressure will be inversely proportional to the calcium ion activity. Ca-Na exchange and precipitation/dissolution of calcium minerals will in turn control the latter parameter. The initial occupancies of exchangeable ions in MX-80 bentonite are well known, but mineral inventories in the bentonite are uncertain due to natural compositional inhomogeneity. One or several of the detected minor minerals may even lack in a particular bentonite supply. Therefore, the effect of the availability of reactive minerals like gypsum and calcite should be investigated, as these minerals will presumably affect pH and porewater composition.

From aqueous extraction tests, BRADBURY and BAEYENS (2002a) inferred the presence of 23.5 mmol/kg of sulphate, which was interpreted as gypsum. On the other hand, MÜLLER-VONMOOS and KAHR (1983) determined 0.7 weight % (70 mmol/kg) calcite in MX-80 bentonite. At the high S/W ratio characterising repository conditions, even these small amounts are sufficient to saturate the aqueous phase with both minerals. To account for the effect of natural variations in minor minerals, we considered the case of porewaters equilibrated with bentonite completely devoid of gypsum, calcite and NaCl.

Table 3.7: Influence of CO_2 partial pressure and availability of minor solids on the composition of bentonite porewaters under repository conditions. All concentrations are given in mol/L. Calcite dissolution and CO_2 escape are indicated by negative numbers, positive numbers denote calcite precipitation and CO_2 uptake. The + sign indicates presence of the minerals in the initial bentonite, the - sign indicates that the mineral was assumed to be absent.

constraints	**(a)**	**(b)**	**(c)**	**(d)**
log pCO_2 / bar	-3.5	-1.5	-3.5	-1.5
calcite	+	+	-	-
gypsum	+	+	-	-
NaCl	+	+	-	-
results	**(a)**	**(b)**	**(c)**	**(d)**
pH	7.8	6.9	7.0	6.9
I	0.32	0.33	0.22	0.23
[Ca]	1.6×10^{-2}	1.3×10^{-2}	4.2×10^{-3}	4.2×10^{-3}
[CO_3]	5.4×10^{-4}	7.2×10^{-3}	7.7×10^{-5}	6.7×10^{-3}
Δ CO_2	4.4×10^{-2}	-3.5×10^{-3}	2.6×10^{-3}	-4.0×10^{-3}
Δ calcite	-4.2×10^{-2}	-1.0×10^{-3}	0	0
[Na]	0.300	0.265	0.195	0.195
[CaZ_2]	0.210	0.191	0.155	0.155
[NaZ]	2.880	2.915	2.979	2.979

The essential results are summarised in Table 3.7. For the cases where the minor solids are assumed to be initially present, we considered calcite and gypsum as saturated phases, while NaCl dissolution was allowed only up to the amount detected (columns 'a' and 'b'). Corresponding calculations where the bentonite is assumed to be devoid of the mentioned minor solids are shown in columns 'c' and 'd'.

The results of the calculations assuming the presence of minor reactive minerals indicate considerable differences in porewater composition, depending on the CO_2 partial pressure. For $pCO_2 = 10^{-3.5}$ bar, the pH increases from 7.3 (reference case calculation) to 7.8. The Ca concentration increases from 13 to 16 mmol/L due to enhanced calcite dissolution and the carbonate concentration drops consequently from 2.8 to 0.5 mmol/L (calcite equilibrium). The enhanced dissolution of calcite also leads to an increased exchange of Ca for Na. Ionic strength and the other concentrations remain almost unchanged. If a high partial pressure of $10^{-1.5}$ bar is assumed, the pH drops to 6.9 and higher carbonate concentrations are obtained. Qualitatively, we can understand the equilibria involved with the help of the following relation, which applies to calcite-saturated system at fixed CO_2 partial pressure:

$$pH = ½ \{ \log K_{sp(calcite)} - \log a_{Ca2+} - \log pCO_2 + A \}$$

where $A \cong +18.2$ is the sum of the decimal logarithms of the dissociation constants for carbonic acid and Henry's constant for CO_2 gas dissolution in water. The relation above predicts a pH decrease of half log unit for an increase of one unit in log pCO_2, at constant calcium ion activity. Since the Ca^{2+} activity is well buffered through gypsum equilibrium and Ca-Na exchange, one successfully predicts a decrease in pH by ~1 unit when log pCO_2 increases from -3.5 to -1.5.

The effect of reactive minerals is best appreciated by comparing calculations 'a' and 'c' ($pCO_2 = 10^{-3.5}$ bar). If calcite and gypsum are lacking, the acidity released through deprotonation of hydroxyl surface species cannot be neutralised through calcite dissolution, and the Ca ions lost through exchange with Na are not compensated by the dissolution of Ca minerals. As a consequence pH and Ca concentration decrease by almost one order of magnitude. Note that the absence of reactions involving calcium minerals leads to considerably smaller mass transfers for CO_2 degassing and Na-Ca exchange. This also has a significant effect on ionic strength (decrease from 0.3 to 0.2 eq./L).

In conclusion, the above calculations indicate that the presence/absence of calcium minerals, in conjunction with the carbonate system, plays an essential role in determining composition and pH of the bentonite porewater. Due to the uncertainties in CO_2 partial pressure and bentonite mineralogy, a rather wide range of possible compositions results for the bentonite porewater. It will therefore be important to study carefully the mineralogical composition and homogeneity of the bentonite supplied for repository construction.

3.5.5 Effects of anion exclusion and reduction of external porosity

Our bentonite porewater model relies on a basic assumption that needs to be discussed and examined in detail. In our model we regard all the water adsorbed by the clay as a single homogeneous aqueous phase. This water is available indistinctly to all dissolved species. In doing that, we ignore: (a) anion exclusion effects due to the negative charge of external clay surfaces, (b) incorporation of water in the structural interlayer of montmorillonite.

Interlayer water is generally considered to be accessible only to exchangeable cations. Anions, uncharged species and other positively charged species are excluded. Consequently, swelling considerably reduces the amount of water available to the latter species and thus the external

porosity (or "geochemical porosity" after PEARSON, 1999). From crystallographic data on the montmorillonite lattice expansion and the constraint of constant volume conditions for bentonite under repository conditions, we were able to estimate that the external porosity will decrease from 38 % to 5 % upon swelling (detailed calculations are given in Appendix B). Our mass balance calculations indicate that 330 of 380 kg water adsorbed per m^3 of dry bentonite will be incorporated as interlayer water, leaving only 50 kg external water.

On the other hand, we could estimate that the average separation of clay particles under such conditions will be less than 3 nm, i.e. less than three times the thickness of the expanded interlayer (see Appendix B). This implies that the properties of the external water will resemble to those of the interlayer water, due to the vicinity of the diffuse double layers of adjoining particles. One may question whether a differentiation between external and internal water is then justifiable, as the physico-chemical properties of two water types will approach at very high compaction. Faced to this dilemma, we decided to follow the conventional model approach and regard all the water adsorbed in the clay as a single homogeneous aqueous phase, in which no distinction is made between external and internal water. Thus, we assumed for our reference calculations that all adsorbed water in bentonite is available to dissolved reactants.

We judged nevertheless essential to perform alternative calculations taking into account the effects of both anion exclusion and reduction of external porosity, in order to assess the impact of the simplifying assumptions made in deriving the reference porewater. To this aim, calculations were performed with a refined model, which accounts explicitly for anion exclusion in the double layer and for the reduction of the external porosity (from 38 % to 5 %). Essentially, these calculations (discussed in detail in Appendix E) indicate that the compositional effects induced by anion exclusion in the diffuse double layer are negligible, whereas the effects of porosity reduction are significant. However, the combined effect does not alter the main characteristics of the porewater in terms of pH and ligand concentrations. Because of this and also considering the uncertainties inherent in the refined model, we decided to retain the original, simplistic model (i.e. without double layer and porosity reduction effects) to define the reference porewater.

3.5.6 Summary

The sensitivity analysis indicates that pH, ionic strength and composition of the porewater resulting from the reaction between Opalinus Clay water and MX-80 sodium bentonite depends critically on the equilibrium partial pressure of carbon dioxide and on the availability of minor calcium minerals (calcite, gypsum). Due to large uncertainties on the value of pCO_2, the pH values in the bentonite porewater may vary between 6.9 and 7.8. The modelling results indicate that, at fixed pCO_2 and in the presence of calcite and gypsum, the bentonite porewater system is well buffered through carbonate equilibria and surface protolysis reactions. Particularly, the system proves to be rather insensitive to the initial speciation of surface hydroxyl sites and to anion exclusion. Variations of the available water volume (external porosity) have a significant effect on porewater composition but do not alter its main character.

4 EVOLUTION OF POREWATER CHEMISTRY

4.1 Modelling approaches

In the previous chapter, porewater chemistry has been assessed for the equilibration of the bentonite with the first pore volume of formation water intruding from the host rock. In this section, we try to estimate the influence of time on bentonite porewater chemistry by modelling diffusive transport of dissolved species from and to the host rock. Two simple models are applied: the "exchange cycle" model (e.g., WANNER, 1986; BRUNO et al., 1999) and a coupled one-dimensional diffusion-reaction model (e.g., ARCOS et al., 2000a; 2000b).

4.1.1 Exchange cycle model

In this model transport is simulated by water exchange cycles. At each cycle, fresh Opalinus Clay water replaces the previously reacted porewater and equilibrates instantaneously with the bentonite. The evolution of porewater chemistry and mineral inventory in the backfill is recorded during a number of exchange cycles.

This approach is the simplest method to estimate the effect of changing site occupancies and mineral inventories on water chemistry. In these calculations the same constraints as for the modelling of the initial saturated conditions in the bentonite are applied (e.g. constant $pCO_2 = 10^{-2.2}$ bar). The calculations were carried out with the PHREEQC code (PARKHURST and APPELO, 1999) using thermodynamic data specified in the Nagra/PSI database, version 05/92 (PEARSON and BERNER, 1991; PEARSON et al., 1992).

The results for major ions, exchangeable species and minerals are presented in Table 4.1. The first cycle corresponds to the initial equilibration derived in section 3.4 by the MINSORB code. Slight differences in the results arise from the different activity correction procedure used in these calculations. The dissolution of gypsum, which strongly affects initial porewater composition, is complete after two exchange cycles. This is accompanied by the displacement of exchanged Na by Ca (Figure 4.1). The changes in calcite content due to dissolution or precipitation are very small compared to the initial inventory (Figure 4.2). In general, the results indicate that the porewater chemistry and exchanged site populations are stabilised after the first exchange cycles. This effect can be explained by the similar chemical and mineralogical properties of Opalinus Clay and MX-80 bentonite and contrasts with previous model calculations performed in the context of the Kristallin-I safety assessment (reaction with Ca-HCO_3 dominated groundwaters from the crystalline basement), where the exchange cycle approach leads to significant changes in porewater chemistry and site occupancies (NAGRA, 1994; WIELAND et al., 1994; BRUNO et al., 1999).

Analogous calculations were carried out also with the limiting pCO_2 values of $10^{-1.5}$ to $10^{-3.5}$ bar. The results for these cases resemble those obtained for a pCO_2 of $10^{-2.2}$ bar, thus indicating that the stabilisation of the porewater composition does not depend on CO_2 partial pressure.

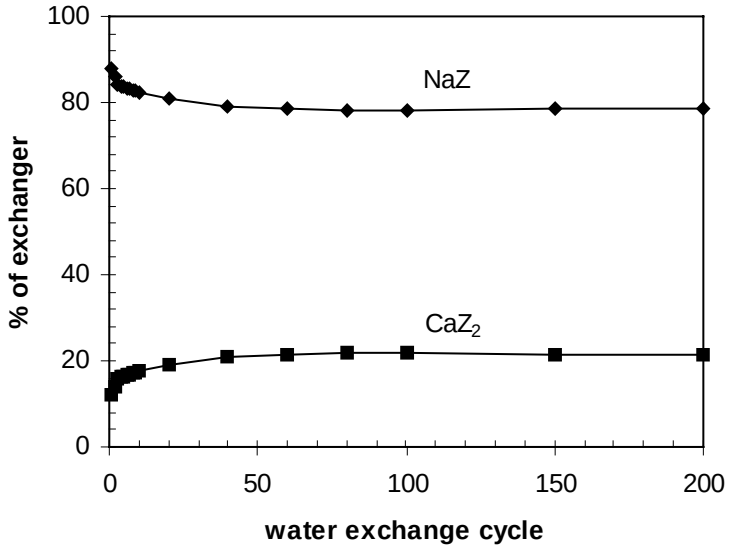

Figure 4.1: Evolution of Na and Ca exchanged ions according to the exchange cycle model.

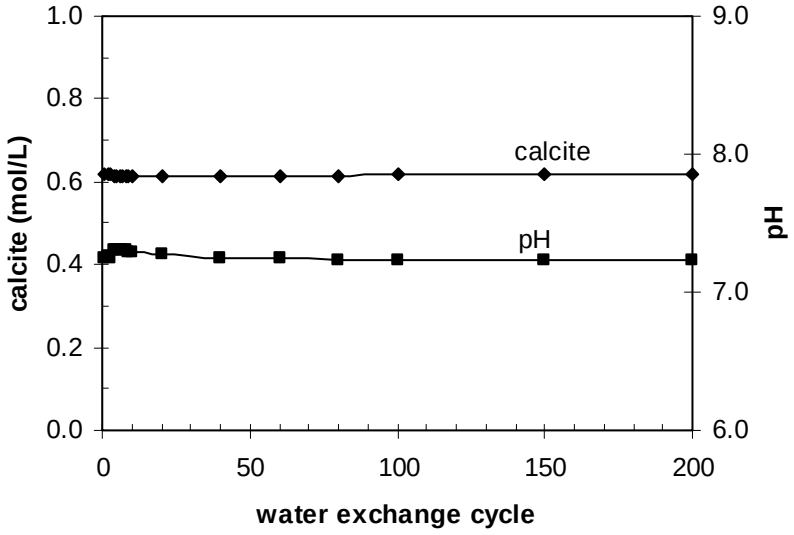

Figure 4.2: Evolution of calcite inventory and pH according to the exchange cycle model.

Table 4.1: Results of water exchange cycle model for $pCO_2 = 10^{-2.2}$ bar.

exchange cycle	**pH**	**Na** mol/L	**Ca** mol/L	**SO_4** mol/L	**CO_3** mol/L	**Cl** mol/L	**NaZ** %	**CaZ_2** %	**gypsum** mol/L	**calcite** mol/L
1	7.25	2.77E-01	1.32E-02	6.27E-02	2.79E-03	1.68E-01	88.0	12.0	0.067	0.618
2	7.26	2.46E-01	1.30E-02	6.15E-02	2.80E-03	1.60E-01	85.9	14.1	0.030	0.617
3	7.25	2.30E-01	1.29E-02	5.36E-02	2.74E-03	1.60E-01	84.2	15.8	0.000	0.618
4	7.30	1.92E-01	7.90E-03	2.40E-02	3.02E-03	1.60E-01	83.8	16.2	0.000	0.615
5	7.31	1.87E-01	7.74E-03	2.40E-02	3.05E-03	1.60E-01	83.6	16.4	0.000	0.615
6	7.31	1.86E-01	7.82E-03	2.40E-02	3.03E-03	1.60E-01	83.3	16.7	0.000	0.615
7	7.30	1.86E-01	7.93E-03	2.40E-02	3.01E-03	1.60E-01	83.1	16.9	0.000	0.615
8	7.30	1.85E-01	8.04E-03	2.40E-02	2.99E-03	1.60E-01	82.9	17.1	0.000	0.615
9	7.30	1.84E-01	8.15E-03	2.40E-02	2.97E-03	1.60E-01	82.7	17.3	0.000	0.615
10	7.29	1.84E-01	8.26E-03	2.40E-02	2.96E-03	1.60E-01	82.5	17.5	0.000	0.615
20	7.27	1.79E-01	9.11E-03	2.40E-02	2.83E-03	1.60E-01	80.9	19.1	0.000	0.615
40	7.25	1.74E-01	1.01E-02	2.40E-02	2.71E-03	1.60E-01	79.2	20.8	0.000	0.615
60	7.24	1.71E-01	1.04E-02	2.40E-02	2.67E-03	1.60E-01	78.5	21.5	0.000	0.615
80	7.24	1.70E-01	1.05E-02	2.40E-02	2.66E-03	1.60E-01	78.4	21.6	0.000	0.616
100	7.24	1.70E-01	1.06E-02	2.40E-02	2.65E-03	1.60E-01	78.3	21.7	0.000	0.616
150	7.24	1.69E-01	1.05E-02	2.40E-02	2.66E-03	1.60E-01	78.4	21.6	0.000	0.617
200	7.24	1.69E-01	1.05E-02	2.40E-02	2.66E-03	1.60E-01	78.4	21.6	0.000	0.618
Opalinus Clay water	7.24	1.69E-01	1.05E-03	2.40E-02	2.70E-03	1.60E-01				

4.1.2 Diffusion-reaction model

In this alternative model the evolution of porewater chemistry is assessed through a one-dimensional diffusion-reaction model integrated in the code PHREEQC, Version 2 (PARKHURST and APPELO, 1999). Transport of a species through the bentonite is described by:

$$\frac{\partial C}{\partial t} = D_e \frac{\partial^2 C}{\partial x^2} - \frac{\partial q}{\partial t}$$

where C (mol/kg porewater) is the species concentration, t is the time (s), x is the distance (m), D_e the effective diffusion coefficient (m^2/s) and q the concentration in the solid phase (mol/kg of porewater). PHREEQC solves the transport part by an explicit finite difference scheme. The chemical interaction term $\partial q/\partial t$ is computed separately for each time step and corresponds to the change in concentration of the solid phase.

Diffusion through the bentonite backfill is treated in the following way: A bentonite column is divided into 6 cells, each 40 cm in length (Figure 4.3). At each end of the column constant boundary conditions, i.e. constant concentrations corresponding to Opalinus Clay water, are imposed. A uniform effective diffusion coefficient of 10^{-10} m^2/s is assumed for all species. The initial conditions in the bentonite column are set by the chemical composition of Opalinus Clay water, and by the initial exchange ion and mineral inventories, as given in Table 3.1. At $t = 0$ the aqueous species start to diffuse through the cells while reacting with the accessory minerals and the clay surface sites (interlayer and edge sites).

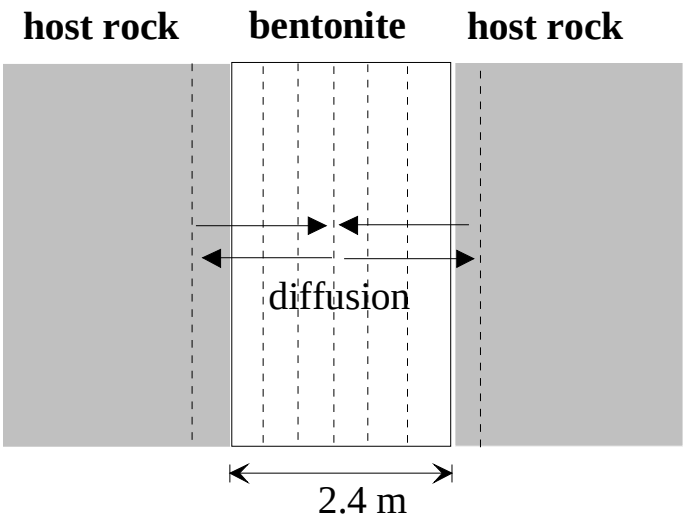

Figure 4.3: One-dimensional diffusion model to represent the evolution of the bentonite porewater in time, explanations in text.

The results of the diffusion-reaction model are shown in Table 4.2 for the cell with its midpoint located at 60 cm distance from the host rock boundary. The evolution of the exchangers NaZ and CaZ_2, of pH and of the calcite inventory for the same cell is also illustrated in Figs. 4.4 and 4.5. The results indicate that during the first thousand years slight changes in the porewater chemistry occur, mainly due to complete dissolution of gypsum and concomitant Na/Ca exchange. After about 5'000 years the compositions are essentially stabilised. These results are similar to those obtained from the exchange cycle model and confirm that only small changes in porewater composition are expected with time.

Table 4.2: Results of diffusion-reaction model: concentrations in central cells (100 cm from Opalinus Clay boundary).

Time years	**pH**	**Na** mol/L	**Ca** mol/L	**SO_4** mol/L	**CO_3** mol/L	**Cl** mol/L	**NaX** %	**CaX_2** %	**gypsum** mol/L	**calcite** mol/L
0	7.25	2.77E-01	1.32E-02	6.27E-02	2.79E-03	1.68E-01	88.0	12.0	0.067	0.618
317	7.25	2.52E-01	1.31E-02	6.13E-02	2.79E-03	1.61E-01	86.3	13.7	0.039	0.617
634	7.28	2.12E-01	9.95E-03	3.76E-02	2.90E-03	1.59E-01	84.3	15.7	0.000	0.616
951	7.31	1.93E-01	7.94E-03	2.65E-02	3.05E-03	1.59E-01	84.1	15.9	0.000	0.615
1'268	7.31	1.89E-01	7.65E-03	2.44E-02	3.07E-03	1.59E-01	83.9	16.1	0.000	0.615
1'585	7.31	1.87E-01	7.71E-03	2.41E-02	3.05E-03	1.59E-01	83.6	16.4	0.000	0.614
1'903	7.31	1.86E-01	7.85E-03	2.40E-02	3.03E-03	1.59E-01	83.3	16.7	0.000	0.614
2'220	7.30	1.85E-01	8.02E-03	2.40E-02	3.00E-03	1.59E-01	83.0	17.0	0.000	0.614
2'537	7.30	1.84E-01	8.19E-03	2.40E-02	2.97E-03	1.59E-01	82.6	17.4	0.000	0.614
2'854	7.29	1.84E-01	8.35E-03	2.40E-02	2.95E-03	1.59E-01	82.3	17.7	0.000	0.614
4'756	7.27	1.79E-01	9.19E-03	2.40E-02	2.82E-03	1.59E-01	80.8	19.2	0.000	0.614
5'074	7.27	1.78E-01	9.30E-03	2.40E-02	2.81E-03	1.59E-01	80.6	19.4	0.000	0.614
6'342	7.26	1.76E-01	9.67E-03	2.40E-02	2.76E-03	1.59E-01	79.9	20.1	0.000	0.614
12'684	7.24	1.71E-01	1.05E-02	2.40E-02	2.67E-03	1.59E-01	78.5	21.5	0.000	0.614
19'026	7.24	1.70E-01	1.06E-02	2.40E-02	2.65E-03	1.59E-01	78.3	21.7	0.000	0.614
22'197	7.24	1.69E-01	1.06E-02	2.40E-02	2.65E-03	1.59E-01	78.3	21.7	0.000	0.614
25'368	7.24	1.69E-01	1.05E-02	2.40E-02	2.66E-03	1.59E-01	78.3	21.7	0.000	0.614
29'807	7.24	1.69E-01	1.05E-02	2.40E-02	2.66E-03	1.59E-01	78.4	21.6	0.000	0.614
OPA-water	7.24	1.69E-01	1.05E-03	2.40E-02	2.70E-03	1.60E-01				

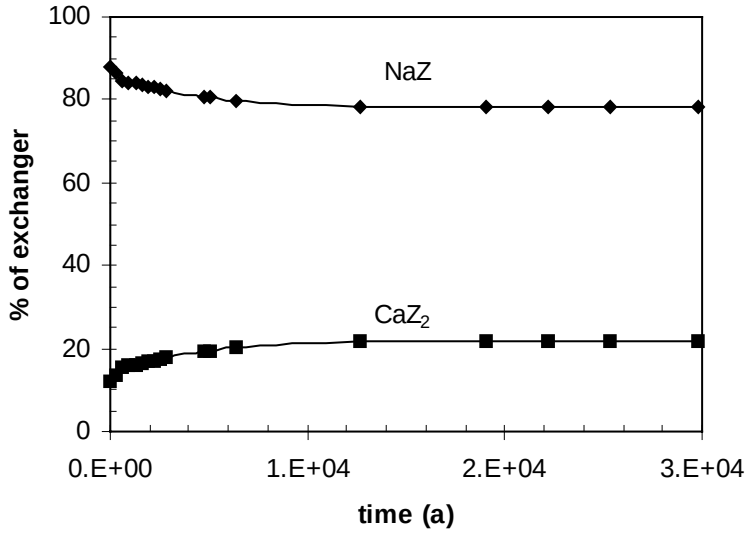

Figure 4.4: Evolution of exchanger composition according to 1-D diffusion reaction model.

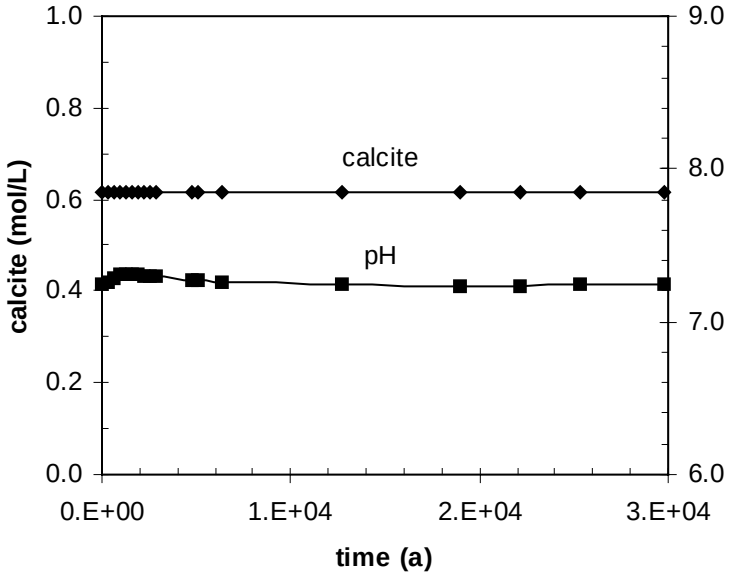

Figure 4.5: Evolution of calcite inventory and pH according to 1-D diffusion-reaction model.

4.2 Model uncertainties

Both models used to describe porewater evolution have important, but unavoidable limitations. We are aware that diffusion through compacted bentonite is very complex and involves physico-chemical effects not accounted for in our model (for example ion-specific diffusivities and the cylindrical geometry of the repository system). Unfortunately, there is to date no appropriate model coupled with chemical reactions, capable to take such effects into account.

In spite of these shortcomings, our models are useful to explore possible trends of porewater evolution under the expected geochemical boundary conditions. In particular, the effects of initial exchanger composition and dissolution/precipitation of reactive minerals can be evaluated. Both models consistently indicate that the initial porewater chemistry will change little over time. This result corresponds to our expectations since the chemical properties of the Opalinus Clay host rock and the MX-80 bentonite are rather similar. On the other hand, in the case of distinct host rock mineralogies, strong changes in porewater chemistry may be predicted with such simple models. For example, the exchange cycle model for the Swedish crystalline repository environment (BRUNO et al., 1999) predicts strong changes in porewater chemistry (e.g. a pH increase of more than 3 units) within a relatively short period. These model calculations were performed under the assumption of a bentonite system closed with regard to pCO_2 exchange, which does not seem appropriate to us for the considered long time scales. In addition, the results obtained by BRUNO et al. (1999) are not supported by geochemical observation on bentonite rocks, where a remarkable chemical stability after formation is observed (GRIM and GÜVEN, 1978).

5 DEFINITION OF THE REFERENCE BENTONITE POREWATER

5.1 Introductory remarks

In this chapter, we define reference bentonite porewater compositions for the determination of radionuclide solubility and sorption parameters in the context of "Entsorgungsnachweis". The reference waters are derived as described in chapter 3, with the addition of the boundary conditions specified by WERSIN et al. (2003) to fix redox conditions. To this aim, the whole model system was set up assuming saturation equilibrium with magnetite and estimated Fe(II) concentrations. Uncertainties in the composition of the reacting groundwater were taken into account by considering (in addition to the reference Opalinus Clay water) two alternative Opalinus Clay waters with carbon dioxide partial pressures fixed $10^{-1.5}$ and $10^{-3.5}$ bar, respectively ("low-pH" and "high-pH", see PEARSON, 2002).

5.2 Redox equilibria

The magnetite equilibrium is taken from the Nagra-PSI thermodynamic database update 01-01 (HUMMEL et al., 2002):

$$Fe_3O_4\,(s) + 8\,H^+ + 2e^- = 3\,Fe^{2+} + 4\,H_2O \qquad \log K^0 = 36.06$$

In order to assess Eh-pH ranges relevant for repository conditions, the bentonite porewaters were modelled at three different fixed CO_2 partial pressures ($10^{-3.5}$, $10^{-2.2}$ and $10^{-1.5}$ bar) associated with three different background concentrations of Fe(II) (8.0×10^{-6}, 4.3×10^{-5} and 7.7×10^{-5} mol/L). These Fe(II) concentrations correspond to the minimum, reference, and maximum concentrations given by PEARSON (2002) for Opalinus Clay water and are fixed by equilibrium with siderite (an important secondary mineral in the Opalinus Clay) at a given pCO_2. Therefore, they cannot be varied independently of pH. The results of our calculations yield three porewater compositions with fixed Eh-values, corresponding to the specified CO_2 partial pressures (Table 5.1 and Table 5.2). All calculated potentials are negative, with the highest potential (-131 mV) obtained at the lowest pH (6.9 for $pCO_2 = 10^{-1.5}$ bar). Figure 5.1 shows the results of the calculations performed to define the range of oxidation potentials in a pH-Eh diagram.

Table 5.1: Derivation of Eh-values in bentonite porewater assuming magnetite/Fe(II) equilibrium. The Fe(II) concentrations are fixed by siderite equilibrium in Opalinus Clay water (PEARSON, 2002).

	reference case	**high pCO_2**	**low pCO_2**
log pCO_2 (bar)	-2.2	-1.5	-3.5
pH	7.3	6.9	7.8
[Fe(II)] (mol/L)	4.3×10^{-5}	7.7×10^{-5}	8.0×10^{-6}
Eh (mV)	-194	-131	-283

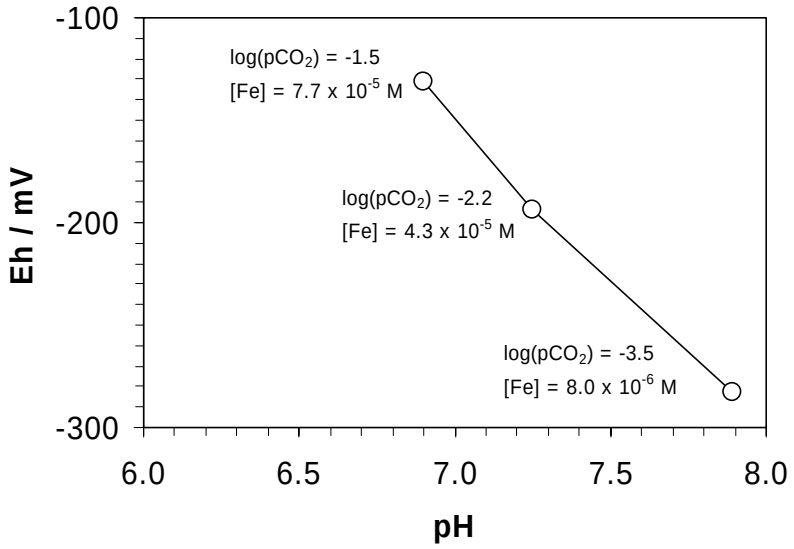

Figure 5.1: Eh-pH diagram for the redox model applied to the reference bentonite porewater system.

An important assumption in our redox model is that sulphate reduction, which generally requires microbial mediation, will not occur under repository conditions. Thus, sulphide-sulphate equilibria have been excluded, implying that pyrite is considered to be inert in our system. Our assumption is corroborated by recent experimental data, which indicate that sulphate-reducing bacteria are not active in compacted bentonite (PEDERSEN et al., 2000).

5.3 Reference bentonite porewater composition

5.3.1 Major elements

Before discussing the resulting reference water compositions, we recall the main results of the modelling work presented in chapter 3 and 4:

- The pH and composition of the bentonite porewater are largely a function of pCO_2. This parameter is at present poorly known.
- Other uncertain parameters, such as the initial distribution of hydroxyl species at the clay surface or the external porosity, have only minor effects on porewater chemistry.
- Only relatively small compositional changes are expected after equilibration of the bentonite with the first groundwater pore volume.

The results are summarised in Table 5.2. For the reference case we assume a pCO_2 of $10^{-2.2}$ bar, consistent with the conditions selected for the Opalinus Clay reference water (PEARSON, 2002). Two alternative compositions, denoted "low pH" and "high pH", define two limiting cases corresponding to the lowest and highest CO_2 equilibrium partial pressures that can be assumed according to our present understanding.

The resulting porewaters are characterised by a net positive or negative charge, arising from the applied surface complexation approach. As discussed in chapter 3.4, counter ions in the double layer are not treated separately in MINSORB and are thus included in the average water composition. However, for some calculations involving radionuclide solubility and sorption it proved more practical to operate with charge balanced porewaters. In these cases, the excess charge was compensated through addition or subtraction of chloride ions. This procedure has little influence on the concentration of chloride itself (maximum increase by 15 %) and of all other solution species.

Table 5.2: Reference bentonite porewater ("D-RBPW") and alternative porewater compositions ("high pH" and "low pH") obtained by fixing pCO_2 at the bounding values.

	low pH	**D-RBPW**	**high pH**
log pCO_2 [bar]	-1.5	-2.2	-3.5
pH	6.90	7.25	7.89
pε	-2.22	-3.27	-4.78
ionic strength [eq/L]	0.356	0.323	0.263
dissolved species [mol/L]			
K	1.67×10^{-3}	1.55×10^{-3}	1.38×10^{-3}
Na	2.91×10^{-1}	2.74×10^{-1}	2.49×10^{-1}
Ca	1.33×10^{-2}	1.32×10^{-2}	1.34×10^{-2}
Sr	3.68×10^{-5}	1.90×10^{-5}	2.92×10^{-6}
Mg	8.91×10^{-3}	7.64×10^{-3}	6.15×10^{-3}
Mn	3.65×10^{-5}	2.34×10^{-5}	4.81×10^{-6}
Fe	7.74×10^{-5}	4.33×10^{-5}	8.00×10^{-6}
Al	1.53×10^{-8}	1.92×10^{-8}	7.55×10^{-8}
Si	1.80×10^{-4}	1.80×10^{-4}	1.84×10^{-4}
SO_4	6.39×10^{-2}	6.16×10^{-2}	5.59×10^{-2}
CO_3	6.99×10^{-3}	2.83×10^{-3}	5.86×10^{-4}
Br	3.00×10^{-4}	2.40×10^{-4}	1.20×10^{-4}
F	1.49×10^{-4}	1.67×10^{-4}	1.59×10^{-4}
Cl	2.06×10^{-1}	1.66×10^{-1}	8.61×10^{-2}
surface species [mol/L]			
=XOH	3.31×10^{-1}	3.25×10^{-1}	2.73×10^{-1}
$=XOH_2^+$	2.07×10^{-2}	9.84×10^{-3}	2.34×10^{-3}
$=XO^-$	1.73×10^{-2}	3.47×10^{-2}	9.36×10^{-2}
=XO(total)	3.69×10^{-1}	3.69×10^{-1}	3.69×10^{-1}
net surface charge	3.38×10^{-3}	-2.48×10^{-2}	-9.13×10^{-2}

Parameter uncertainties that may be relevant for solubility or sorption calculations are discussed briefly below:

- **Carbonate**: The uncertainty in total and free carbonate concentrations is closely linked to the assumed pCO_2. A range between 0.6 and 7 mmol/L can be specified from the two boundary cases given in Table 5.2.
- **pH**: The uncertainty of pH values (6.9 to 7.9) is also closely related to the assumed pCO_2 (see boundary cases given in Table 5.2).
- **Eh**: The predicted range (-283 to -131 mV) is determined by magnetite equilibrium and background Fe(II) concentration (Table 5.1).
- **Chloride**: Cl^- concentrations in the bentonite porewater are largely determined by chloride dissolved in the Opalinus Clay water (about 0.17 mol/L). Dissolution of salt impurities in bentonite only slightly affects this concentration.
- **Sulphate**: Concentrations are significantly affected by the dissolution of sulphate impurities. Gypsum and calcite saturation will limit SO_4^{2-} concentrations to a very tight range (60-64 mmol/L). Over time, the initial gypsum inventory will be totally dissolved and sulphate concentrations will approach those of OPA water (about 10 mmol/L).

5.3.2 Trace elements

Impurities in the bentonite and in the Opalinus Clay water may affect radionuclide migration. In particular, radionuclide speciation may be adversely influenced by dissolved ligands, such as phosphate or fluoride. In addition, background concentrations of safety relevant elements (e.g. Ni, Co, Cs, U, Th) can be important in limiting the concentration of radionuclides dissolved from the waste to levels below the elemental solubility (solubility sharing effect, see NAGRA, 1994). In the following, we report and comment available trace element data for bentonite and Opalinus Clay.

Bentonite

There are a few published chemical data available. Of interest is the study performed by VOGT and KÖSTER (1978) on various bentonite standard materials, also including Wyoming bentonite standards. We also include some unpublished data on MX-80 analyses kindly provided by ANDRA (E. GIFFAULT, pers. communication). Table 5.3 lists trace element data from these studies. The high levels of phosphate, Ba and Sr (> 100 ppm) are probably related to undetected trace solids (phosphates, barite, celestite) since these elements are strongly concentrated in the non-clay fraction. Noteworthy are also the elevated concentrations of some metals, such as Zn and Zr.

Opalinus Clay

There is a considerable amount of data from the Mont Terri rock laboratory (SCHOLTIS et al., 1999). Table 5.4 lists trace elements in porewater derived from their compilation.

Table 5.3: Trace element concentrations (ppm) in Wyoming bentonite standards and commercial MX-80 bentonite.

	commercial MX-80	**Upton Wyoming USA**		**Clay Spur Wyoming USA**	
sample	raw bentonite	raw bentonite	*montmorillonite fraction*	raw bentonite	*montmorillonite fraction*
Reference	ANDRA (unpubl.)	Vogt and Köster (1978)			
Method	ICP-MS[1]	XRF	*XRF*	XRF	*XRF*
Cr	30	5	*2*	n.d.	*3*
Mn	155	77	*12*	30	*37*
P	600	127	*37*	138	*40*
Cu	5	3	*1*	1	*2*
Ni	4	25	*20*	14	*19*
Co	1	5	*26*	24	*14*
Pb	50	46	*21*	51	*20*
Zn	90	106	*172*	120	*162*
Rb	16	24	*19*	27	*19*
Li		26	*10*	26	*10*
Sr	290	165	*39*	85	*27*
Ba	325	258	*23*	194	*22*
Ti	1000	660	*660*	720	*660*
As	15				
Be	2				
Bi	1				
Cd	1				
Ce	100				
Cs	0.5				
Dy	8				
Er	4				
Eu	0.7				
Ga	28				
Gd	8				
Ge	0.6				
Hf	8				
Ho	2				
In	0.1				
La	48				
Lu	0.5				
Mo	5				
Nb	26				
Nd	45				
Pr	12				
Sb	2				
Sm	10				
Sn	10				
Ta	4				
Tb	1				
Th	42				
Tm	0.6				
U	15				
V	6				
W	0.3				
Y	40				
Yb	4				
Zr	192				

1: average from 3 samples

Table 5.4: Trace element concentrations in Opalinus Clay porewater at Mont Terri.

Element	**conc.** (mol/L)	**Source**
As	< 3E-07	1a
Ba	3E-07	1a
Be	<3E-10	1b
Bi	2E-09	1b
Cd	<9E-09	1b
Ce	<1E-8	1b
Co	<6E-09	1a
Cr	<4E-08	1a
Cs	5E-08	1a
Dy	1E-09	1b
Eu	<4E-08	1b
Er	1E-08	1b
F	5.4E-5	1c
Gd	<5E-08	1b
Hf	2E-08	1b
Ho	4E-09	1b
La	<4E-09	1b
Li	1E-04	1b
Lu	4E-09	1b
Mn	4E-06	1b
Mo	<3E-08	1a
Nb	7E-09	1b
Nd	2E-09	1b
Ni	<9E-08	1a
P	3E-5	1a
Pb	<5E-08	1b
Pr	<2E-08	1b
Rb	4E-07	1b
Sb	3E-09	1b
Sm	1E-08	1b
Sn	4E-09	1b
Ti	2E-05	1b
Tm	<2E-09	1b
Th	1E-09	1b
U	4E-09	1b
Y	4E-08	1b
Yb	3E-09	1b
Zn	2E-06	1a
Zr	4E-08	1b

Sources: 1a: SCHOLTIS et al. (1999), Table 4.2.6; average conc. from 3 samples
1b: SCHOLTIS et al. (1999), Table 4.2.7, average conc. from 3 samples
1c: SCHOLTIS et al. (1999), Table 4.2.3, one measurement

6 CONCLUSIONS

The porewater chemistry in the bentonite backfill has been defined for a repository emplaced in the Opalinus Clay formation by applying a thermodynamic model that takes recent experimental results into account. This relatively simple model has been shown to adequately describe experimental data up to S/W ratios of 1.5 kg/L. The model has been then applied to predict the initial porewater composition in the compacted bentonite, which required extrapolation to S/W ratios of 4.5 kg/L. A sensitivity analysis has been carried out to identify critical physico-chemical parameters and to define the ranges of possible porewater compositions. The evolution of porewater chemistry with time has been explored with two alternative models, one assuming sequential porewater exchange cycles, the second based on one-dimensional diffusion. The two models yield very similar results, indicating only minor compositional changes with time. Finally, a redox model has been integrated and three bentonite porewater compositions (a reference and two boundary compositions) have been derived. Effects related to anion exclusion in the double layer and to the reduction of the external porosity have been investigated by means of a refined model. However these processes have not been implemented in the model applied to derive the reference porewater compositions, due to the large conceptual uncertainties involved.

The results of the sensitivity analysis indicate that the bentonite system has a high acid-base buffering capacity, provided by reactions involving protonation-deprotonation of the surface hydroxyl sites and above all by the carbonate system (through calcite equilibrium and CO_2 exchange with an external reservoir). Because of the similar chemical and mineralogical properties of bentonite and Opalinus Clay, the modelled bentonite porewater does not differ greatly from the reacting groundwater. For the same reason, the bentonite porewater composition is predicted to remain stable for very long times. The main geochemical uncertainty arises from the poorly known partial pressure of CO_2 in the surrounding host rock. In contrast, other uncertain parameters (e.g. initial distribution of hydroxyl surface species, mineral inventories) and processes neglected in the reference porewater model (e.g. anion exclusion in the double layer) are predicted to have a minor influence on porewater composition.

The thermodynamic models used in this study do not consider some complex physico-chemical processes specifically occurring in compacted swelling clays (e.g. osmosis, reduction of the dielectric constant of water). These processes are still poorly understood and cannot yet be considered quantitatively in geochemical calculations. Further experimental investigations and new methodologies need to be developed to improve geochemical modelling for such systems. Nevertheless, we are confident that our analysis is sufficiently realistic and that the derived reference porewater composition is suitable for performance assessment applications.

Acknowledgements

Urs Berner, Bart Baeyens, Mike Bradbury, Lawrence Johnson, Bernhard Schwyn, Ian McKinley and Ingeborg Hagenlocher are acknowledged for many useful discussions and review work. We are also very thankful to Tony Appelo whose careful review and suggestions largely helped to improve this report. Finally, we thank Christine Bircher for the editorial work.

7 REFERENCES

AECL (1994): The disposal of Canada's nuclear fuel waste: the vault model for postclosure assessment, Atomic Energy of Canada Limited Report AECL-10714, COG-93-4, AECL, Pinawa, Canada.

ALLARD, B., LARSON, S.A. et al. (1981): Minerals and precipitates in fractures and their effects on the retention of radionuclides in crystalline rocks. Proceedings of "Near-field phenomena in geologic repositories for radioactive waste", Seattle, 1981. ISBN 92-64-02236-8.

ANDERSSON, J. (1999): SR 97: Data and data uncertainties. Compilation of data and data uncertainties for radionuclide transport calculations. SKB Technical Report TR-99-09, SKB, Stockholm, Sweden.

ARCOS, D., BRUNO, J., BENBOW, S., TAKASE, H. (2000a): Behaviour of bentonite accessory minerals during the thermal stage. SKB Technical Report TR-00-06, SKB, Stockholm, Sweden.

ARCOS, D., BRUNO J., DURO, L., GRIVÉ, M. (2000b): Desarrollo de un modelo geoquímico de campo próximo. ENRESA Publicación técnica 4/2000, ENRESA, Madrid, Spain.

BAEYENS B., BRADBURY M.H. (1995): A quantitative mechanistic description of Ni, Zn and Ca sorption on Na-Montmorillonite. Part I: Physico-chemical characterisation and titration measurements. PSI Report 95-10, Waste Management Laboratory, Paul Scherrer Institut, Villigen, Switzerland and Nagra NTB 95-04, Nagra, Wettingen, Switzerland.

BATEMAN, K., ENTWISLE, D.C., KAMP, S., SAVAGE, D. (1991): Bentonite-groundwater interactions: results from compression rig experiments. Nagra Internal Report.

BATEMAN, K., ENTWISLE, D.C., KEMP, S., SAVAGE, D. (1996): Bentonite-groundwater interactions: results of compression rig experiments. Nagra Internal Report.

BEAUCAIRE, C., PITSCH, H., TOULHOAT, P., MOTELLIER, S., LOUVAT, D. (2000): Regional fluid characterisation and modelling of water-rock equilibria in the Boom clay formation and in the Rupelian aquifer at Mol, Belgium. Applied Geochemistry 15, 667-686.

BENBOW, S., SAVAGE, D., WERSIN, P., JOHNSON, L.H. (2000): Modelling thermal alteration of bentonite barriers in Opalinus Clay. Silica migration - SiO_2 and smectite kinetics, Nagra Internal Report.

BORKOVEC, M., WESTALL, J. (1983): Solution of the Poisson-Boltzmann equation for surface excesses of ions in the diffuse layer at the oxide-electrolyte interface. J. Electroanal. Chem. 150, 325-337.

BRADBURY, M.H., BAEYENS, B. (1994): Sorption by Cation exchange. Incorporation of a cation exchange model into geochemical computer codes. PSI Report 94-07, Waste Management Laboratory, Paul Scherrer Institut, Villigen, Switzerland and Nagra NTB 94-11, Nagra, Wettingen, Switzerland.

BRADBURY, M.H., BAEYENS, B. (1995): A quantitative mechanistic description of Ni, Zn and Ca sorption on Na-montorillonite. Part III: Modelling. PSI Report 95-12, Waste

Management Laboratory, Paul Scherrer Institut, Villigen, Switzerland and Nagra NTB 95-06, Nagra, Wettingen, Switzerland.

BRADBURY, M.H., BAEYENS, B. (1997): A mechanistic description of Ni and Zn sorption on Na-montmorillonite. Part II: modelling. J. Contam. Hydrol. 27, 223-248.

BRADBURY, M.H., BAEYENS, B. (1998): A physico-chemical characterisation and geochemical modelling approach for determining porewater chemistries in argillaceous rocks. Geochimica et Cosmochimica Acta 62, 783-795.

BRADBURY, M.H., BAEYENS, B. (2002a): Porewater chemistry in compacted re-saturated MX-80 bentonite. PSI Report 02-10, Waste Management Laboratory, Paul Scherrer Institut, Villigen, Switzerland and Nagra NTB 01-08, Nagra, Wettingen, Switzerland.

BRADBURY, M.H., BAEYENS, B. (2002b): A comparison of D_a and K_d values deduced from diffusion experiments in compacted Kunigel V1 bentonite with those derived from batch sorption measurements: A case study for Cs(I), Ni(II), Sm(III), Am(III), Zr(IV) and Np(V). Nagra NTB 02-17, Nagra, Wettingen, Switzerland.

BRUNO, J., ARCOS, D., DURO, L. (1999): Processes and features affecting the near field hydrochemistry. Groundwater-bentonite interaction. SKB Technical Report TR-99-29, SKB, Stockholm, Sweden.

CHOI, J.-W., OSCARSON, D.W. (1996): Diffusive transport through compacted Na- and Ca-bentonite. J. Contam. Hydrol. 22, 189-202.

CUEVAS, J., VILLAR, M.V., FERNÁNDEZ, P., GÓMEZ, P., MARTÍN, P.L. (1997): Porewaters extracted from compacted bentonite subjected to simultaneous heating and hydration. Applied Geochemistry 12, 473-481.

CURTI, E. (1993): Modelling bentonite porewaters for the Swiss high-level radioactive waste repository. PSI Report 93-05, Waste Management Laboratory, Paul Scherrer Institut, Villigen, Switzerland and Nagra NTB 93-45, Nagra, Wettingen, Switzerland.

CURTI, E. (1997): Coprecipitation of radionuclides: basic concepts, literature review and first applications. PSI Report 97-10, Waste Management Laboratory, Paul Scherrer Institut, Villigen, Switzerland and Nagra NTB 97-08, Nagra, Wettingen, Switzerland.

DEGUELDRE, C., SCHOLTIS, A., LAUBE, A., TURRERO, M.J., THOMAS, B. (2003): Study of the pore water chemistry through an argillaceous formation: a paleohydrochemical approach. Applied. Geochem. 18, 55-73.

GRAUER, R. (1986): Bentonit als Verfüllmaterial im Endlager für hochaktiven Abfall: Chemische Aspekte. EIR-Report Nr. 576, Swiss Federal Institute for Reactor Research (now Paul Scherrer Institut, Villigen, Switzerland) and Nagra NTB 86-12, Nagra, Wettingen, Switzerland.

GRAUER, R. (1990): The chemical behaviour of montmorillonite in a respository backfill: selected aspects. Nagra NTB 88-24E, Nagra, Wettingen, Switzerland.

GRAUER, R. (1993): Zum Verhalten der technischen Barrieren in einem Endlager für hochaktiven Abfall. Internal Technical Note AN-44-93-04, Waste Management Laboratory, Paul Scherrer Institut, Villigen, Switzerland.

GRIM, R.E., GÜVEN, N. (1978): Bentonites: geology, mineralogy, properties and uses. Developments in Sedimentology 24, Elsevier, Amsterdam.

HORSEMAN, S.T., HIGGO, J.J.W., ALEXANDER, J., HARRINGTON, J.F. (1996): Water, gas and solute movement through argillaceous media. Report CC-96/1, Nuclear Energy Agency, OECD, Paris, France.

HUMMEL, W., BERNER, U., THOENEN, T., CURTI, E., PEARSON, F.J. (2002): Nagra / PSI Chemical Thermodynamic Data Base 01-01. Nagra NTB 02-16, Nagra, Wettingen, Switzerland and Universal Publishers/uPublish.com, ISBN 1-58112-620-4, Parkland, Florida, USA, 565 p.

JNC (1999): H12 Project to establish technical basis for HLW disposal in Japan. Supporting report 3. Safety assessment, Japan Nuclear Cycle Development Institute JNC/TN1400 99-013, JNC, Japan.

JOHNSON, L.W., SCHNEIDER, J.W. (2000): Preliminary parameter values for SPENT. Nagra Internal Report.

KAHR, G., KRAEHENBUEHL, F., MÜLLER-VONMOOS, M., STOECKLI, H.F. (1986): Wasseraufnahme und Wasserbewegung in hochverdichtetem Bentonit. Nagra NTB 86-14, Nagra, Wettingen, Switzerland.

KARABORNI, S., SMIT, B., HEIDUG, W., URAI, J., VAN OORT, E. (1996): The swelling of clays: molecular simulations of the hydration of montmorillonite. Science 271, 1102-1104.

LEMIRE, R.J., GARISTO, F. (1989): The solubility of U, Np, Pu, Th and Tc in a geological disposal vault for used nuclear fuel. Atomic Energy of Canada Limited Report, AECL-10009, AECL, Pinawa, Canada.

MATTIGOD, S.V., SPOSITO, G. (1978): Improved method for estimating the standard free energies of formation ($\Delta G^0_{f,298.15}$) of smectites. Geochim. Cosmochim. Acta 42, 1753-1762.

MAY, H.M., KINNIBURGH, D.G., HELMKE, P.A., JACKSON, M.L. (1986): Aqueous dissolution, solubilities, and thermodynamic stabilities of common aluminosilicate clay minerals: Kaolinite and smectites. Geochim. Cosmochim. Acta 50, 1667-1677.

MELAMED, A., PITKÄNEN, P., OLIN, M., MUURINEN, A., SNELLMAN, M. (1992): Interaction of water and compacted sodium-bentonite in simulated nuclear waste disposal conditions. Mat. Res. Soc. Symp. Proc. 257, 557-566.

MÜLLER-VONMOOS, M., KAHR, G. (1983): Mineralogische Untersuchungen von Wyoming Bentonit MX-80 und Montigel. Nagra NTB 83-12, Nagra, Wettingen, Switzerland.

MUURINEN, A., LEHIKOINEN, J. (1999): Porewater chemistry in compacted bentonite. POSIVA report 99-20, POSIVA OY, Helsinki, Finland.

MUURINEN, A., PENTILLA-HILTUNEN, P., RANTANEN, J., UUSHEIMO, K. (1987): Diffusion of uranium and chloride in compacted Na bentonite. Report YJT-87-14. Nuclear waste Commission of Finnish Power Companies, Helsinki, Finland.

NAGRA (2002): Project Opalinus Clay. Safety report. Nagra NTB 02-05, Nagra, Wettingen, Switzerland.

NAGRA (1994): Kristallin-I: safety assessment report. Nagra NTB 93-22, Nagra, Wettingen, Switzeland.

NAUNDORF, W., WOLLENBERG, R. (1992): Herstellung von Bentonit-Granulat mit hoher Schüttdichte zur Bohrlochabdichtung. Nagra NTB 92-06, Nagra, Wettingen, Switzerland.

NEA (2000): Porewater extraction from argillaceous rocks for geochemical characterisation. Methods and interpretations. Nuclear Energy Agency, OECD, Paris, France.

ODA, C., SHIBATA, M., YUI, M. (1999): Calculation of porewater chemistry for the 2nd progress P.A report, JNC Technical Report; referenced in H12, supporting report 3, safety assessment, Japan Nuclear Cycle Development Institute JNC/TN1400 99-013, JNC, Japan.

OSCARSON, D.W. (1994): Surface diffusion: Is it an important transport mechanism in compacted clays? Clays Clay Mineral. 42, 534-543.

OSCARSON, D.W., DIXON, D.A. (1989): Elemental, mineralogical, and pore-solution compositions of selected Canadian clays. Atomic Energy of Canada Limited Report, AECL-9891, AECL, Pinawa, Canada.

PARKHURST, D.L., APPELO, C.A.J. (1999): User's guide to PHREEQC (Version 2) - A computer program for speciation, batch reaction, one-dimensional transport, and inverse geochemical calculations. U.S. Geological Survey Water-Resources Investigations Report 99-4259, Denver (CO), USA.

PEARSON, F.J., BERNER, U. (1991): Nagra thermochemical database - I. Core data. Nagra NTB 91-17, Nagra, Wettingen, Switzerland.

PEARSON, F.J., BERNER, U., HUMMEL, W. (1992): Nagra thermochemical database - II. Supplemental data 05/92. Nagra NTB 91-18, Nagra, Wettingen, Switzerland.

PEARSON, J.F., SCHOLTIS, A., GAUTSCHI, A., BAEYENS, B., BRADBURY, M., DEGUELDRE, C. (1999): Chemistry of Porewater. In: Mont Terri Rock Laboratory. Results of the hydrogeological, geochemical and geotechnical experiments performed in 1996 and 1997 (eds. M. Thury, P. Bossart). Landeshydrologie und -geologie Geologische Berichte Nr. 23, Bern , Switzerland, pp. 129-147.

PEARSON, F.J. (1999): What is the porosity of a mudrock? In: Aplin, A.C., Fleet A.J., Macquaker J.H.S. (eds), Muds and mudstones: Physical and fluid flow properties. Geological Society, London, Special Publications, Vol. 158, pp. 9-21.

PEARSON, F.J. (2002): Benken Reference Water Chemistry. Nagra Internal Report.

PEDERSEN, K., MOTAMEDI, M., KARNLAND, O., SANDÉN, T. (2000): Cultivability of microorganisms introduced into a compacted bentonite buffer under high-level radioactive waste repository conditions. Engineering Geology 58, 149-161.

POSIVA (1999): Safety assessment of spent fuel disposal in Hästholmen, Kivetty, Olkiluoto and Romuvaara. TILA-99, by T. Vieno and H. Nordman. Posiva 99-07, Posiva, Helsinki, Finland.

SATO, H., ASHIDA, T., KOHARA, Y., YUI, M., SASAKI, N. (1992): Effect of dry density on diffusion of some radionuclides in compacted sodium bentonite. J. Nucl. Sci. Techn., 29, 873-882.

SATO, H., YUI, M., YOSHIKAWA, H. (1995): Diffusion behavior for Se and Zr in sodium-bentonite. Mat. Res. Soc. Symp. Proc. 353, 269-276.

SATO, H., YUI, M. (1997): Diffusion of Ni in compacted bentonite. J. Nucl. Sci. Tech. 34 (3), 334-336.

SATO, H. (1998): Diffusion behaviour of Se(-II) and Sm(III) in compacted sodium bentonite. Radiochim. Acta 82, 173-178.

SCHOLTIS, A., DEGUELDRE, C., TURRERO, M.J., LAUBE, A., BAUER-PLAINDOUX, C., STEIGER, H. (1999): WS-A experiment: Water- & gas sampling and isotopic raw data (26^{th} to 28^{th} August 1998) for: boreholes BWS-A1, -A2 and -A3 Murchisonae-Concava-beds spring, Jurensis marl spring. Mont Terri Project, unpublished Technical Note 99-16, Federal Office of Water and Geology, Bern, Switzerland.

SKB (1999): Deep repository for spent nuclear fuel. SR 97 - Post-closure safety. Main Report, volume 1. SKB Technical Report TR-99-06, SKB, Stockholm, Sweden.

SNELLMAN, M., UOTILA, H., RANTANEN, J. (1987): Laboratory and modelling studies of sodium bentonite groundwater interaction. Mat. Res. Soc. Symp. Proc. 84, 781-790.

SPOSITO, G., PROST, R. (1982): Structure of water adsorbed on smectites. Chemical Reviews 82, 553-573.

TARDY, Y., DUPLAY, J. (1992): A method of estimating the Gibbs free energies of formation of hydrated and dehydrated clay minerals. Geochim. Cosmochim. Acta 56, 3007-3029.

TARDY, Y., FRITZ, B. (1981): An ideal solid solution model for calculating solubility. Clay Minerals 16, 361-373.

THOENEN, T. (2000): The effect of a reduced dielectric constant of water at clay mineral surfaces on ion association and complexation. Internal Technical Note AN-44-00-10, Waste Management Laboratory, Paul Scherrer Institut, Villigen, Switzerland.

TSIPURSKY, S.I., DRITS, V. (1983): The distribution of octahedral cations in the 2:1 layers of dioctahedral smectites studied by oblique-texture electron diffraction. Clay Minerals 19, 177-193.

VOGT, K., KÖSTER, H.M. (1978): Zur Mineralogie, Kristallchemie und Geochemie einiger Montmorillonite aus Bentoniten. Clay Minerals 13, 25-43.

WANNER, H. (1986): Modelling interaction of deep groundwaters with bentonite and radionuclide speciation. EIR-Report 589, Paul Scherrer Institut, Villigen, Switzerland and Nagra NTB 86-21, Nagra, Wettingen, Switzerland.

WANNER, H., WERSIN, P., SIERRO, N. (1992): Thermodynamic modelling of bentonite-groundwater interaction and implications for near field chemistry in a repository for spent fuel. SKB Technical Report TR-92-37, SKB, Stockholm, Sweden.

WANNER, H., ALBINSSON, Y., KARNLAND, O., WIELAND, E., WERSIN, P., CHARLET, L. (1994): The acid/base chemistry of montmorillonite. Radiochim. Acta 66/67, 157-162.

WERME, L. (1992): unpublished data, presented in Wanner et al. (1992).

WERSIN, P., JOHNSON, L.H., SCHWYN, B., BERNER, U., CURTI, E. (2003): Redox conditions in the near field of a SF/HLW and an ILW repository in Opalinus Clay. Nagra NTB 02-13, Nagra, Wettingen, Switzerland (in review).

WIELAND, E., WANNER, H., ALBINSSON, Y., WERSIN, P., KARNLAND, O. (1994): A surface chemical model of the bentonite-water interface and its implications for modelling the near field chemistry in a repository for spent fuel. SKB Technical Report TR-94-26, SKB, Stockholm. Sweden.

YU, J.-W., NERETNIEKS, I. (1997): Diffusion and sorption properties of radionuclides in compacted bentonite. SKB Technical Report TR-97-12, SKB, Stockholm, Sweden.

APPENDIX A Modelling of the initial "fresh water" solution used in the experiments of MUURINEN AND LEHIKOINEN (1999)

Introduction

The modelling of the analytical data reported by MUURINEN and LEHIKOINEN (1999) (Table 3.2) revealed, for both initial and final solutions, strong oversaturation with respect to calcite. In addition, the comparison of initial and post-reaction concentrations indicates mass imbalances. Unfortunately, the authors do not give any comment on these topics. In this Appendix, we present some details and guesswork to help understanding the origin of such inconsistencies.

Calcite oversaturation and CO_2 degassing

In the footnote of Table 1 of MUURINEN and LEHIKOINEN (1999), the initial reacting solution ("fresh water") is described as "Allard water … in the glove box conditions". An inquire to the authors (MUURINEN, pers. comm.) revealed that the "fresh water" was prepared outside the glove box according to the recipe of ALLARD et al. (1981), then transferred into a CO_2-free glove box, where pH was measured and carbonate determined via alcalimetric titration. The pH measured in the glove box was 9.1, while the carbonate concentration was 1.8 mM.

Inspection of the composition given in ALLARD et al. (1981) (Table 2, solution "f") reveals that freshly prepared "Allard water" has a pH of 8.2 and a total carbonate concentration of 2.0 mM. Our speciation calculations indicate that this water is saturated with calcite but has a CO_2 overpressure ($pCO_2 = 10^{-3}$ bar) with respect to atmospheric conditions. Thus, in the open atmosphere "Allard water" would degas until equilibrium with atmospheric CO_2 is reached. The pH would drift to 8.7, if no calcite precipitation occurs (SI = 0.5)[1], or to 8.5 if calcite precipitates. In the latter case, however, 20 mg calcite per L solution would form, an event that can hardly escape experimental observation. According to MUURINEN (pers. comm.) no precipitate was observed at any stage of the experiments. From this, we conclude that the solution was effectively oversaturated[2].

If the above solution is transferred to the CO_2-free glove box in an open bottle, degassing will proceed up to consumption of all dissolved carbonate, ultimately yielding a carbonate-free solution with pH 11.3. The pH of 9.1 measured by MUURINEN and LEHIKOINEN (1999) implies thus only partial degassing, possibly indicating that the vessels were not tight. We calculated that 0.2 mmol CO_2 /L must escape to reach a pH of 9.1. This amount corresponds exactly to the difference between total carbonate concentration (123 mg/L or 2.0 mmol/L) given by ALLARD et al., 1981) and that determined in the glove box (1.8 mmol /L) by MUURINEN and LEHIKOINEN (1999).

The results above strongly suggest that the solutions used by the Finnish authors partially degassed in the glove box, thereby leading to strongly oversaturated, but apparently stable, solutions.

---

[1] This equilibrium is reached after loss of a very small amount of CO_2, leaving unchanged the total carbonate concentration in solution, and should therefore be quite fast. Note that a significant pH drift would occur also in a closed bottle if it is not filled completely.

[2] An explanation for the metastability may be found in the literature on calcite coprecipitation experiments (CURTI, 1997). In the laboratory, calcite oversaturated solutions appear to be stable in the absence of solids. As soon as calcite crystal seeds are added, precipitation starts instantaneously. Since both initial solution and "external water" in the experiments of MUURINEN and LEHIKOINEN (1999) were not in contact with any mineral, it is conceivable that these solutions could persist metastably.

Mass balance calculations

Mass balance calculations for major elements are presented in Table A-1, based on the analytical results given by MUURINEN and LEHIKOINEN (1999) for the reaction between "fresh water" solution and MX-80 bentonite at 1.5 kg/L. The solution and exchange data reported in Table A-1 correspond to those reported in Table 3.2, but are expressed in mmol/L and complemented with mass transfer data for the relevant gas and solid phases.

Table A-1: Mass balance calculations for the modelled Finnish experiment (fresh water + MX-80 bentonite at 1.5 kg/L) reported in Table 3.2. Experimental data are given in normal typeface, modelled data in italics. Differences (Δ) are percentages relative to final totals. Analytical values were taken from Table 1 and Appendices A1 and A4 of MUURINEN and LEHIKOINEN (1999).

concentrations [mmol/L]		**solution**	**exchanged**	**minor solids**	**total**
Na^+	initial	2.26	909	4.22[a]	915.5
	final	247	729	*0*	976
					Δ = + 6 %
Ca^{2+}	initial	0.464	72.0	86.9[b] + 224.8[c]	384.2
	final	9.06	98.3	*33.2*[d] *+ 209.3*[e]	*349.9*
					Δ = - *10* %
Mg^{2+}	initial	0.19	30.9	-	31.1
	final	4.0	33.8		37.8
					Δ = + 18 %
K^+	initial	0.1	10.1	-	10.2
	final	1.71	10.5		12.2
					Δ = + 16 %
CEC	initial		750		
[meq./kg]	final		669		
			Δ = -12 %		
CO_3^{2-}	initial	1.8	-	224.8[c]	*226.6*
	final	3.6		*209.3*[e] *+ 14.8*[f]	*227.7*
					Δ = + *0.5* %
SO_4^{2-}	initial	0.10	-	86.9[b]	*87.0*
	final	129		*33.2*[d]	*162.2*
					Δ = + *46* %
Cl^-	initial	1.48	-	*4.22*[a]	*5.7*
	final	5.7			*5.7*
					Δ = *0* %

[a] calculated from the difference in the analytical Cl^- concentrations of initial and final waters
[b] corresponds to 0.58 w % $CaSO_4$ (Table 2 in MUURINEN and LEHIKOINEN, 1999) at S/W=1.5 kg L^{-1}
[c] corresponds to 1.5 w % $CaCO_3$ (Table 2 in MUURINEN and LEHIKOINEN, 1999) at S/W=1.5 kg L^{-1}
[d] results from dissolution of 53.7 mmol/L gypsum (calculated with Model 1)
[e] results from dissolution of 15.5 mmol/L calcite (calculated with Model 1)
[f] amount of CO_2 (g) degassed (calculated with Model 1)

The mass balance for calcium, carbonate, sulphate and chloride cannot be set up with experimental data alone, since changes in mineral inventories and gas phase affecting the mentioned species have not been tracked analytically. Dissolved amounts of calcite, gypsum and NaCl, as well as CO_2 degassing had thus to be determined through geochemical modelling. In contrast, the balances for sodium, magnesium and potassium rely entirely on experimental data and can be used to assess the accuracy of the measurements. For the latter elements, imbalances between 6 % and 18 % of the total amounts were found. These discrepancies cannot be explained only by analytical uncertainties in the solution concentrations but are rather related to uncertainties in the determination of exchange cation populations (750 vs. 669 meq/kg as initial and final cation exchange capacities). Such uncertainties of ~ 10 % are within the expected range for such determinations and are thus acceptable.

The imbalances of +46 % for sulphate and -10 % for calcium can be readily explained with uncertainties in the inventories of calcium minerals. For carbonate, we note an almost perfect mass balance. Thus, also for these species mass balances are acceptable, considering the unavoidably large uncertainties involved in the determination of minor solids.

APPENDIX B Residual external porosity and separation of clay particles in saturated compacted bentonite under repository conditions

Residual porosity after resaturation of compacted MX-80

KAHR et al. (1986, Figure 11) determined experimentally the expansion of the c*-axis[1] lattice parameter for montmorillonite separated from MX-80 bentonite, as a function of the gravimetric water content. Such measurements can be used to evaluate the volume increase of expandable clay minerals following incorporation of water in the structural interlayer (swelling). The interlayer of smectites can adsorb up to four sheets of water molecules (GRAUER, 1986) and hosts exchanged cations. These counterbalance the negatively charged TOT (SiO_4-MO_6-SiO_4) units. Interlayer water (also denoted interlamellar water) has physico-chemical properties differing from those of water residing between clay particles (interparticle water) and is generally considered as part of the crystal structure of montmorillonite.

Assuming constant bulk volume conditions, a residual porosity can be calculated, representing the ratio of external water volume (i.e. volume occupied by water not incorporated in the structural interlayer of montmorillonite) to bulk bentonite volume after swelling has occurred. If the bulk densities of dry and saturated bentonite[2] (ρ_{dry}, ρ_{wet}) are known, it is possible to determine the external water content after swelling (w). One starts with the definitions:

$$\rho_{dry} = \frac{m_s}{V_b} \qquad \text{and} \qquad \rho_{wet} = \frac{m_s + m_w}{V_b} \ , \tag{B-1}$$

where m_s is the mass of dry mineral in the bentonite, m_w is the total mass of adsorbed water and V_b is the bulk bentonite volume. For constant volume conditions, the following relation applies:

$$\frac{m_s}{\rho_{dry}} = \frac{m_s + m_w}{\rho_{wet}} \tag{B-2}$$

from which one obtains (noting that $w \equiv \frac{m_w}{m_s}$):

$$w = \frac{\rho_{wet}}{\rho_{dry}} - 1 \tag{B-3}$$

Substituting the reference values for the dry and wet bentonite densities (1711.2 and 2091.2 kg m^{-3}, see JOHNSON and SCHNEIDER, 2000) yields $w = 0.222$. Taking into account the presence of 25 % accessory minerals in MX-80 bentonite, we end up with the water content of $w^* = 0.296$, normalised to the weight of pure montmorillonite.

---

[1] The c* axis is perpendicular to the (001) plane and thus slightly differs from the crystallographic c axis.(see Figure B-1)

[2] The dry density is the bulk density of dried bentonite granulates (water contents below 1 weight %), obtained after drying at 135°C for about ½ hour (see NAUNDORF and WOLLENBERG, 1992). This residual initial water can be neglected in the present calculations. The saturated density is the reference bulk density after resaturation with water under constant volume conditions.

From Figure 11 in KAHR at al. (1986) one extracts $d_0 \approx 9.66$ Å and $d \approx 16.5$ Å for the d-spacing before and after swelling, respectively. The relative volume increase of the solid phase, $\Delta V_s / V_s^0$, is then:

$$\frac{\Delta V_s}{V_s^0} = x_M \frac{d - d_0}{d_0} \approx 53.5\ \% \qquad \text{(B-4)}$$

where $x_M = 0.755$ is the volume fraction of montmorillonite in MX-80 (which is taken here to be equal to the weight fraction, due to the similar densities of the mineral phases, see MÜLLER-VONMOOS and KAHR, 1983). The volume of dry mineral per unit volume of bentonite is given by:

$$V_s^0 = \frac{\rho_{dry} V_b}{\rho_s} = \frac{1711.2 \times 1}{2760} \approx 0.62\ \text{m}^3 \qquad \text{(B-5)}$$

which yields an initial porosity (ε_{dry}) of 0.38. This represents the air-filled fraction of the bulk bentonite volume prior to water saturation. The volume of solid after the 53.5 % expansion due to the water saturation process is then 0.62 x (1 + 0. 535) = 0.952 m^3, leaving a residual porosity of 0.048. Thus, our calculation predicts that about 85 % of the initial physical porosity is destroyed by the swelling process. This residual porosity is however much larger than the through-diffusion porosities derived from chloride diffusion experiments for compacted bentonite, which are less than 1 % (MUURINEN et al., 1987).

Volume balance calculations

The volumetric changes can be calculated with the help of following balance equation, applied before and after swelling:

$$V_b = V_{ext} + V_{\text{int}} + V_{TOT} + V_{acc}\,. \qquad \text{(B-6)}$$

V_b is the bulk bentonite volume, V_{ext} is the external porosity volume, V_{int} is the interlayer space, V_{TOT} is the (constant) volume of TOT sheets and V_{acc} is the volume of accessory minerals. Following expressions account for the different volumes:

$$V_{\text{int}} = (1 - \varepsilon_{dry})\, V_b \left[\sigma\, \rho_{dry}\, h + x_M \left(\frac{d - d_0}{d} \right) \right] \qquad \text{(B-7)}$$

where $\sigma = 2.81 \times 10^5$ m^2 / kg is the internal surface area of bentonite (MÜLLER-VONMOOS and KAHR, 1983)[3], and h = 0.73 Å is the separation between adjoining TOT sheets before swelling. This parameter corresponds to the separation of basal oxygen planes, as measured with the help of the crystal structure visualisation program DIAMOND V2.1 using the montmorillonite structure model of TSIPURSKY and DRITS (1983).

[3] MÜLLER-VONMOOS and KAHR (1983) calculated an internal area of 749 m^2/g for MX-80 montmorillonite, which rescales to 562 m^2/g for the bulk bentonite due to the presence of 25 % accessory minerals. The latter number is the sum of both sides of the internal surface and must therefore divided by 2 in our calculations, yielding an effective surface area of 281 m^2/g.

$$V_{TOT} = (1-\varepsilon_{dry})\, V_b \left[\, x_M - \sigma\, \rho_{dry}\, h \right] \quad \text{(B-8)}$$

$$V_{acc} = (1-\varepsilon_{dry})\, V_b \left[\, 1 - x_M \right] \quad \text{(B-9)}$$

$$V_{ext} = V_b - V_{\text{int}} - V_{TOT} - V_{acc} \quad \text{(B-10)}$$

Applying the equations above to a bentonite block of V_b = 1 m^3 yields the volumes listed in Table B-1. From these numbers, one derives a mass of ~ 49 kg for the water filling the residual external porosity (assuming a density of 1000 kg m^{-3}). The mass of water trapped in the interlayer space can be derived by subtracting the 49 kg of external water from the total amount of water adsorbed, m_w, which can be computed by combining eqs. B-2 and B-5:

$$m_w = \left(1-\varepsilon_{dry}\right)\rho_s V_b \left(\frac{\rho_{wet}}{\rho_{dry}} - 1\right) = 380 \text{ kg.} \quad \text{(B-11)}$$

This leaves 331 kg of water in the interlayer space.

The interlayer space is occupied by water molecules and exchanged cations. The volume occupied by exchanged cations, V_{ex}, can be estimated as follows for MX-80 bentonite containing a homoionic sodium montmorillonite:

$$V_{ex} = \{x_M \rho_s (1-\varepsilon_{dry})\, V_b CEC\} \times \{N_A \frac{4}{3}\pi r^3\} = 0.003 \text{ m}^3 \quad \text{(B-12)}$$

A cation exchange capacity (*CEC*) of 0.787 eq./kg and an ionic radius, $r = 1.02 \times 10^{-10}$ m, for the sodium ion were assumed in the calculation above. This implies that the volume fraction occupied by exchanged cations is negligible compared to the total interlayer volume (0.353 m^3). The calculated density of water in the interlayer space, $\rho_{w,\text{int}}$, is then:

$$\rho_{w,\text{int}} = \frac{331\ kg}{0.353\ m^3} = 938\ kg\ m^{-3} \quad \text{(B-13)}$$

Table B-1: Volumetric balance in dry and saturated MX-80 bentonite for 1 m^3 block of compacted bentonite.

	external porosity V_{ext}	interlayer space V_{int}	TOT sheets V_{TOT}	accessory minerals V_{acc}	bulk volume V_b
dry bentonite	0.380	0.022	0.446	0.152	1.000
saturated bentonite	0.049	0.353	0.446	0.152	1.000

Taking into account this calculated water density and assuming that each water molecule occupies an area of 3.5 x 3.5 nm^2 one determines almost exactly 3 monolayers of adsorbed water, which is consistent with the three hydration steps observed by KAHR et al. (1986) during the clay expansion (op. cit., p.15 and Figure 11).

The density calculated for water adsorbed in the interlayer is less than for water under normal conditions. This agrees with experimental evidence indicating that interlayer water is not close-packed, but has a wider "ice-like" structure (see Figure 13 in GRAUER, 1986; and SPOSITO and PROST, 1982). The 30 % water content calculated from the dry and wet density data is thus consistent with the independent x-ray measurements indicating the formation of three water layers (KAHR et al., 1986) and also with the results of molecular simulations, which indicate a water content of ~20 % at 15.5 Å d-spacing (KARABORNI et al., 1996).

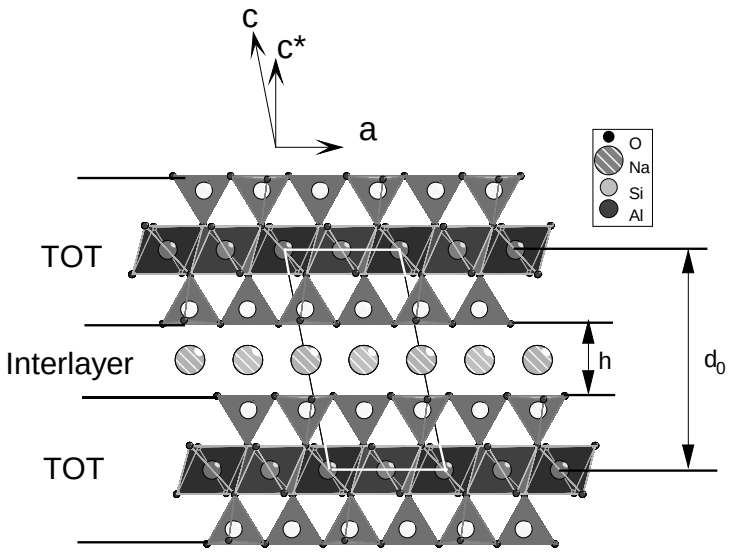

Figure B-1: Structure of dry montmorillonite projected on the (a,c) plane, showing one interlayer and two TOT structural units as well as the unit cell. The crystallographic parameters h and d_0, used in calculations, are indicated. Note that d_0 is not identical to the c_0 lattice parameter because montmorillonite is monoclinic (c_0 is represented through the long segment of the unit cell).

Separation of clay particles in compacted saturated bentonite

We also tried to estimate the average separation between clay platelets, i.e. the average width of the external porewater channels, through which dissolved species are supposed to diffuse and react like in a free solution. We estimated this average separation, δ, as a function of particle size, *a*, by subdividing a sample volume of 1 m^3 of swelled bentonite in *N* equally sized and equally spaced isometric particles of dimension a^3 (Figure B-2).

For a maximum particle size of 0.2 µm, determined for the dry montmorillonite used in the mineralogical analysis (MÜLLER-VONMOOS and KAHR, 1983), the calculated number of particles is:

$$N = \frac{V_b - V_{ext}}{a^3} = \frac{1 - 0.049}{(2 \times 10^{-7})^3} = 1.18875 \times 10^{20} \qquad \text{(B-14)}$$

The average particle separation is then given by the total length of water-filled gaps divided by the number of gaps along any of the three equivalent dimensions (cubic geometry is assumed):

$$\delta = \frac{\sqrt[3]{V_b} - \sqrt[3]{V_b(1-\varepsilon_{res})}}{\sqrt[3]{N} - 1} = \frac{1 - \sqrt[3]{0.951}}{4.917 \times 10^6} = 3.4 \times 10^{-9}\, m \qquad \text{(B-15)}$$

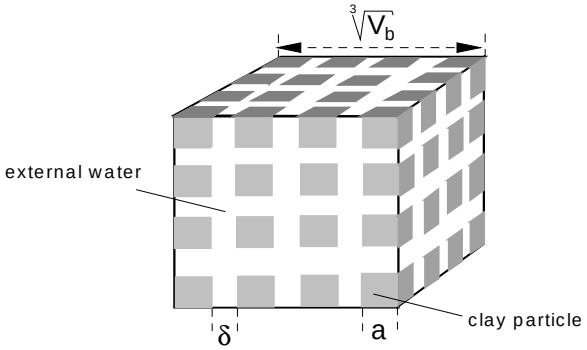

Figure B-2: Conceptual model for the estimation of average separation of swelled clay particles within a bentonite block of volume V_b.

Equation (B-15) is plotted in Figure B-3, where particle separation is given as a function of the assumed particle dimension for MX-80 bentonite compacted under the conditions specified above. According to MÜLLER-VONMOOS and KAHR (1983), more than 90 % of the montmorillonite particles in MX-80 are found in the fraction < 0.2 μm. For this threshold grain size, our calculation predicts an average distance of 3.4 nm between adjoining clay particles in the swelled, compacted bentonite (point 3 in Figure B-3). This corresponds to about 10 water monolayers and is only twice the thickness of the expanded interlayer unit (which is about 1.5 nm thick).

For an aqueous solution with ionic strength around 0.2 - 0.3 mol/L, the Debye length is only about 0.5 nm, leaving a thickness of 2.9 nm for water unaffected by electrostatic surface fields induced by the DDL (see Appendix E). This result implies that interlayer and interparticle water would have distinct properties even at such high compaction degrees, and that the major part of the external water is expected to behave (chemically and physically) like free water. In other words, our basic assumption that chemical reactions in the external water will still proceed like in "beaker experiments" would seem justified in the light of the these calculations.

However, the majority of the particles in MX-80 will have dimensions below 2 μm. Figure B-3 shows that the particle separation rapidly drops to values comparable to the thickness of the expanded interlayer if the grain size is reduced to 1 μm. Point 2 in Figure B-3 indicates the required grain size in order for the external water films to reach equal thickness as the interlayer. This critical size is at about 0.7 μm. Below point 2 the calculations become meaningless, since particle separation becomes smaller than the thickness of the expanded interlayer (region 1 in the figure).

In conclusion, our calculations indicate that most of the external water is subject to electrostatic effects (overlapping DDL's). Therefore the distinction between external solution and water incorporated in the interlayer region of the montmorillonite structure, which is obvious in diluted clay suspensions, becomes unsharp. The chemical properties of such water films are poorly known and cannot be assimilated to a bentonite porewater model with the current knowledge (see also comments in Appendix C).

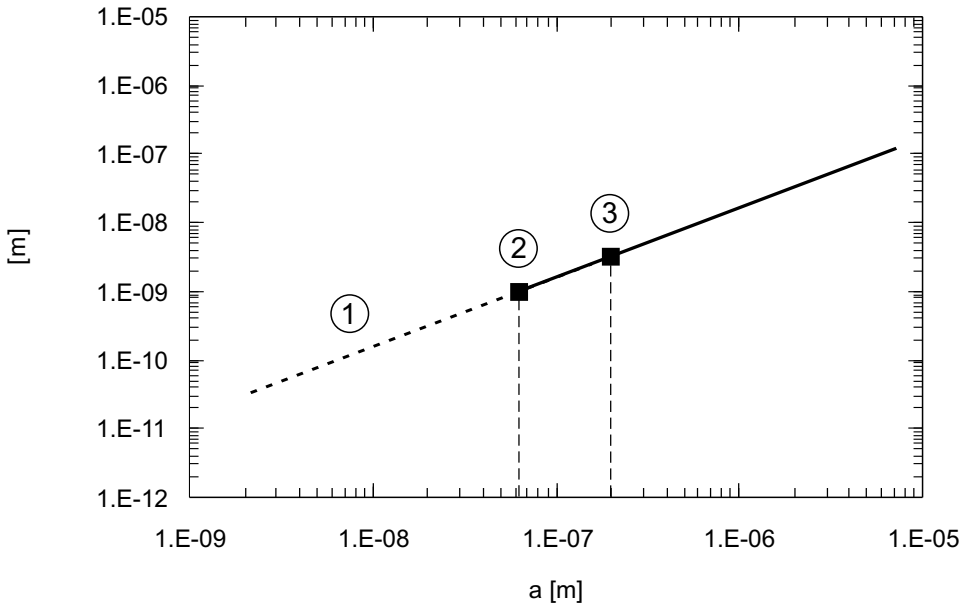

Figure B-3: Plot of particle separation vs. assumed dimension of the clay particles, calculated after equation B-15. See text for explanation.

APPENDIX C Critical issues related to conventional geochemical models

Introduction

In the past years, the limitations of conventional geochemical models applied to compacted saturated clays have become evident. Recent "state-of-the-art" syntheses on water-clay interactions in argillaceous rocks (HORSEMAN et al., 1996) and on laboratory data of porewater extraction tests (NEA, 2000) show that important physico-chemical effects, which can be safely neglected in diluted suspensions, may play a major role in dense saturated clays. These are still not implemented in bentonite porewater models, due to the limitation of current knowledge and to the complexity of the processes involved.

Although it is not within the scope of the present study to give a detailed overview, this report would be incomplete without a brief discussion of the processes that could potentially affect the porewater chemistry in compacted bentonites.

Reduction of external porosity and particle separation

A key process, which could have important consequences on the porewater chemistry of compacted bentonites, is swelling. Through swelling water is incorporated in the interlayer structure of clay minerals, i.e. in the expandable, ~10-20 Å thick zone separating the TOT sheet units of montmorillonite, where the exchanged cations reside. In the terminology used by HORSEMAN et al. (1996), this water is called *interlamellar water* but in this report we prefer the term *interlayer water* to indicate that the water is incorporated in the homonymous structural entity of montmorillonite. Interlayer water must be distinguished from the *external water* residing outside clay mineral particles. Interlayer water is characterised by a low degree of freedom ("ice-like" structure?), anion exclusion and immobility of the solvated cations.

As discussed in Appendix B, swelling in compacted clays leads to an extensive reduction of the amount of external water and drastically reduces the separation between clay particles. Thus the "geochemical porosity" (see PEARSON, 1999), which represents the effective amount of water available to freely mobile dissolved species, is also strongly reduced, and most of the pore water in the clay will be subject to the influence of surface charge. Since conventional thermodynamic equilibrium programs have been designed and calibrated to quantify reactions in free water, there is no guarantee that the thermodynamic constants coded in such programs will hold also for the water affected by electrostatic fields. In Appendix B we have shown that the usual distinction between interlayer and external water may be questioned at high compaction.

Our calculations, based on x-ray diffraction measurements of the d-spacing in MX-80 montmorillonite as a function of the water content (KAHR et al., 1986), yield a residual external porosity of 5 % for a bentonite with 38 % porosity in the dry state (see Appendix B). Through-diffusion experiments with ^{36}Cl (MUURINEN et al., 1987), on the other hand, indicate porosities of less than 1 % for compacted MX-80 bentonite at dry densities of about 1.7 kg L^{-1} (the reference value for the Swiss repository), suggesting that the amount of true external water is extremely small. Based on these observations, BRADBURY and BAEYENS (2002a) calculate a bentonite porewater composition normalised to a water content of a few mL per kg bentonite.

Osmotic effects

Another process not accounted for by conventional geochemical models is chemical osmosis. Compacted clays act as semi-permeable membranes (see chapter 10 in HORSEMAN et al., 1986). In the ideal case, only water molecules would move into compacted bentonite during resaturation, with the important consequence that the bentonite would react with pure water. However, compacted clays are not ideal semi-permeable membranes and - as shown by the chloride diffusion experiments - must have preferential paths through which charged species can diffuse. It remains therefore unclear how osmosis will affect porewater chemistry.

Dielectric constant

A third issue arises from the decrease of the dielectric constant of water, which can be related to the reduced mobility of water molecules in the double layer (THOENEN, 2000). The decrease of the dielectric constant could have far reaching consequences on both diffusion and chemical equilibria. In particular, the formation of uncharged and low-charge complexes would be favoured, since electrostatic interactions between anions and cations become stronger. The use of equilibrium constants determined in ordinary aqueous systems may therefore be inappropriate to model reactions in the porewater fraction subject to DDL effects, as suggested by measurements of complexation constants in ethanol-water mixtures (THOENEN, 2000).

Final remarks

The picture emerging from the considerations above is that of an extremely complex system. Clearly, a great deal of additional experimental and theoretical understanding is needed to account for the mentioned processes in bentonite porewater models. For safety assessment purposes, one is forced to rely to conventional modelling until the effects of such processes on porewater chemistry are sufficiently understood. It is nevertheless possible to estimate the potential effect of some of these processes by means of parameter variations and sensitivity analyses.

APPENDIX D Relations between selectivity coefficients and exchange constants

Consider the generic ion exchange reaction

$$z_A\ B^{z_B} + z_B\ AX_{z_A} = z_B\ A^{z_A} + z_A\ BX_{z_B}$$

where z_A and z_B are the charges of the exchangeable cations *A* and *B*, respectively. The (conditional) equilibrium is defined through the selectivity coefficient

$${}^{B}_{A}K_c \equiv \frac{N_B^{z_A}\ a_A^{z_B}}{N_A^{z_B}\ a_B^{z_A}}.$$

$N_A^{z_B}, N_B^{z_A}$ are the sorbed cation concentrations expressed as equivalent fractions and $a_A^{z_B}, a_B^{z_A}$ are ionic activities in solution. In order to model clay-water interactions with the help of speciation codes, the amounts of ions sorbed on the clay must be related to the solution volume. Hence selectivity coefficient must be converted into exchange constants, defined as

$${}^{B}_{A}K_{ex} \equiv \frac{Q_B^{z_A}\ a_A^{z_B}}{Q_A^{z_B}\ a_B^{z_A}}.$$

$Q_A^{z_B}, Q_B^{z_A}$ are the sorbed cation concentrations expressed in mol/L. Of the two equilibrium expressions, only the selectivity coefficient represents a thermodynamic constant, since exchange constants for heterovalent equilibria (K_{ex} values) depend on S/W ratio and cation exchange capacity (BRADBURY and BAEYENS, 1994):

$${}^{B}_{A}K_{ex} \quad = \quad {}^{B}_{A}K_c\ (CEC)^{z_A - z_B}\ \frac{z_A^{\ z_B}}{Z_B^{\ z_A}}\ (S/W)^{z_A - z_B}$$

Thus, the values of the selectivity coefficients for mono-divalent exchange listed in Table 3.1 must be transformed according to the equation above, yielding: ${}^{Ca}_{Na}K_{ex}$ = 0.37, ${}^{Mg}_{Na}K_{ex}$ = 0.31, ${}^{Sr}_{Na}K_{ex}$ = 0.37. In contrast, the exchange constants for homovalent exchange reactions are independent of CEC and S/W ratio and numerically identical to the corresponding selectivity coefficients. Thus: ${}^{K}_{Na}K_{ex}$ = 4.0 and ${}^{H}_{Na}K_{ex}$ = 1.0. These constants refer to the CEC and S/W ratios relevant to the HLW repository conditions (see Table 3.1).

APPENDIX E A refined bentonite porewater model with explicit inclusion of the diffuse double layer and porosity reduction

Introduction

In the procedure adopted to model the reference bentonite porewaters, no distinction was made between diffuse double layer (DDL) and external solution. This simplifying assumption leads to "average" solutions with a net electrical charge, which is equal in magnitude (but opposite in sign) to that developed on external clay surfaces through deprotonation or protonation of surface hydroxyl groups.

A more realistic model should however differentiate between the uncharged external solution and the diffuse double layer. The external solution is considered to determine radionuclide solubility, since dissolved species can diffuse freely through it and because no electrostatic field modifies the solvent properties. The DDL is a nanometre-thick zone adjacent to the edge surface and is characterised by an excess of cations or anions compensating the surface charge (Figure E-1). The concentrations of cations and anions in this zone differ from those in the external solution in such a way that the net charge of the DDL exactly compensates the surface charge. As a result of this ionic segregation, the composition of the uncharged external water (and thus radionuclide solubilities) may also be affected.

Following a reviewer's suggestion, we refined our porewater model and evaluated compositional effects on the external pore water induced by the explicit calculation of cation excesses in the DDL. Such calculations were carried out by implementing the in-built model of BORKOVEC and WESTALL (1983) in the current version of PHREEQC (PARKHURST and APPELO, 1999). This model relies on Poisson-Boltzmann's equation, which relates surface potential to charge density in the DDL, and results in the combined calculation of both diffuse layer and external solution compositions. There are nevertheless important simplifications and limitations in the PHREEQC implementation of Borkovec and Westall's model, summarised as follows:

1) The thickness of the DDL (Debye length) is fixed during the calculation and is not adjusted automatically to ionic strength and electrolyte composition. This adjustment can in principle be made by manual iteration, but the program crashed when we tried to do it.
2) In the calculation, the amount of water associated to the DDL (the product of Debye length and surface area) is added to the reference amount of bulk solution (1 kg H_2O). In compacted systems, this modifies the effective S/W ratio, which must therefore be adequately corrected on input.
3) It is assumed that speciation in the DDL is the same as in the bulk solution, which is probably not correct due to changes in the dielectric constant of water near the surface (see discussion in Appendix C).
4) Calculated DDL compositions do not always converge to meaningful results, particularly for Debye lengths below 1 nm (this problem is explicitly mentioned in the PHREEQC manual).

Calculations with and without the explicit determination of the DDL composition have been performed for the same experimental system modelled in section 3.3 ("fresh" water reacting with MX-80 bentonite at 1.5 kg/L) and then extended to the reference porewater system (Opalinus Clay water reacting with MX-80 bentonite at 4.5 kg/L). All calculations were carried out with selectivity and surface complexation parameters corresponding to Model 1 (see Table 3.3). The CEC and initial exchanged site occupancies were taken from Table 3.3 for the

experiments of MUURINEN and LEHIKOINEN (1999) and from Table 3.1 for the reference porewaters. It was not possible to implement DDL calculations with Model 2, because this model requires charge-independent surface complexation constants: although PHREEQC offers the option of calculations without the electrostatic term, this option cannot be used in conjunction with an explicit DDL calculation.

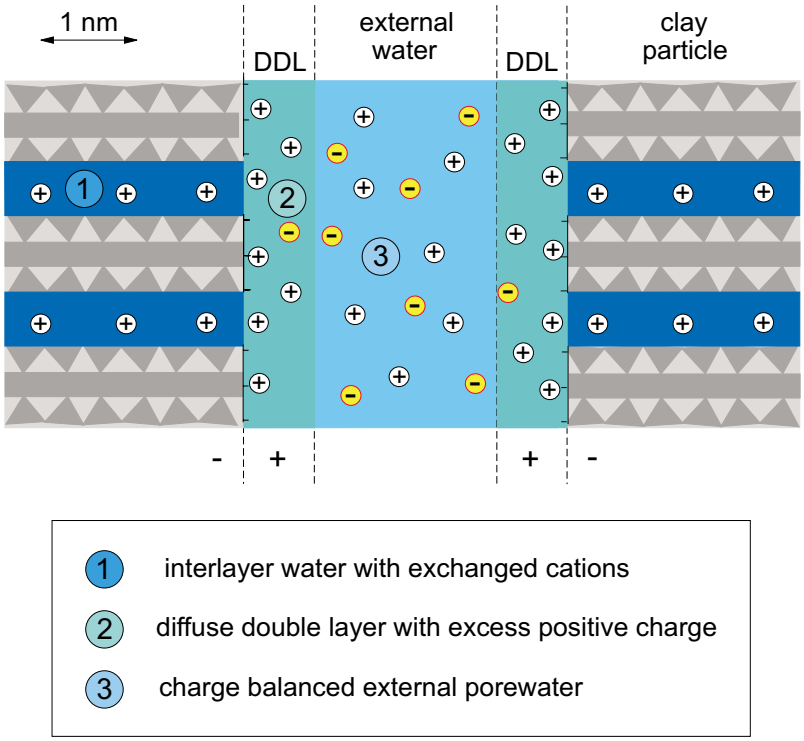

Figure E-1: The different water types in a bentonite-water system.

Outline of model calculations

Our model refinement follows this general scheme:

a) In a first step, a very small amount of pure water with some dissolved NaCl reacts with the initial clay, yielding a tiny amount of solution in equilibrium with the exchanged cations in the bentonite. Since the amount of water is exceedingly small, the initial inventories of minor solids (calcite, gypsum, quartz, kaolinite) and exchanged cations are not modified by this procedure.

b) This solution, which represents a hypothetical native "formation water" in equilibrium with the initial clay, is then rescaled to 1 kg water solvent.

c) The surface site distribution and DDL composition in equilibrium with this 1 kg "formation water" is then calculated. The resulting amount of chloride in the DDL should correspond to the inventory of 1.35 mmol/kg clay (if needed, the amount NaCl given in the first step must be adjusted).

d) The initial clay with the so-calculated surface (including the DDL) and the reactive minor solids (calcite, gypsum, quartz and kaolinite) is then equilibrated with the reacting solution (either "fresh water" or Opalinus Clay water), yielding the required bentonite porewater.

Note that in this model development we assume an initial surface that is different from that used previously. Instead of assuming all edge sites initially being in the $=XOH^0$ state, an initial surface in equilibrium with a hypothetical "formation water" is used. This pre-equilibrated surface is non-unique, since additional constraints influencing the pH and hence edge site protonation could be imposed in step one (e.g. a fixed pCO_2). In section 3.5 we showed that the initial protonation state of the external surface has little influence on the final composition of the pore water, and this finding was confirmed by test calculations applied to the model scheme described above.

Results referring to the Finnish experiments

The results obtained from calculations referring to the Finnish experiment ("fresh" water reacting with MX-80 bentonite at 1.5 kg/L, see Table 3.4) are summarised in Table E-1. The table shows the analytical values before and after reaction on the left side, along with the predictions obtained from three model calculations, all performed with the fixed saturation index of 0.9 for calcite and $10^{-3.2}$ bars pCO_2 as indicated by the analytical data. In addition, a soluble chloride content corresponding to 0.01 weight % NaCl was assumed, as indicated by MUURINEN and LEHIKOINEN (1999).

The first model calculation was carried out without consideration of the DDL composition, assuming that all the water present in the system is available to dissolved species. It corresponds thus to the "Model 1" calculation of Table 3.4. All model results are in the same order of magnitude of the experimental data, but some elemental concentrations (particularly Na, Cl and sulphate) are underpredicted by a factor of two, which leads to a correspondingly lower ionic strength.

The second calculation differs from the previous one by the explicit determination of the DDL composition. It therefore reveals the net effect of counter ions segregation on the composition of the external solution. The results indicate a barely significant effect. Ionic strength, pH, and elemental concentrations are modified by just a few percents with respect to the calculation without consideration of the DDL. Note that the average Na concentration in the DDL is by about a factor of three higher than in the bulk solution, while the Cl concentration is three times lower. The insensitivity of the external water composition to ionic segregation in the DDL is explained by the small amount of water in the DDL compared to the amount of electrically neutral solution.

Table E-1: Model calculations for the reaction between "fresh water" and MX-80 bentonite at S/W= 1.5 kg L^{-1} compared with the analytical values as given by MUURINEN and LEHIKOINEN (1999). The same degree of calcite oversaturation (SI=0.9) and CO_2 overpressure (pCO_2 =$10^{-3.2}$ bar) like in the experiment were assumed for the model calculations.

	Analyses		**Model calculations**		
	Initial	**post-reaction**	**no DDL**	**with DDL, all water external**	**with DDL, 28 % interlayer water**
solution [mmol / kg H_2O]					
Na	2.3	247	110	113	125
K	0.1	1.7	0.7	0.8	0.7
Mg	0.2	4.0	3.0	3.2	3.6
Ca	0.5	9.1	10.4	10.4	10.2
Cl	1.5	5.7	3.5	3.7	5.7
CO_3	1.8	3.6	2.7	2.7	2.8
SO_4	0.1	133	65.8	66.4	70.0
ionic strength	0.004	0.330	0.172	0.176	0.190
pH	9.1	8.4	8.3	8.3	8.3
exch. ions [eq. fraction]					
NaZ	0.808	0.719	0.714	0.722	0.752
CaZ_2	0.128	0.194	0.228	0.219	0.189
MgZ_2	0.055	0.077	0.050	0.051	0.051
KZ	0.009	0.010	0.008	0.008	0.008
CEC [eq. kg^{-1}]	0.750	0.675	0.750	0.750	0.750
edge sites [eq. fraction]					
$=XOH_2^+$			~ 0	0.002	0.003
=XOH			0.026	0.198	0.229
$=XO^-$			0.974	0.800	0.767
net charge [meq. / kg H_2O]			-41.5	-36.7	-55.8
DDL [mmol/ kg H_2O]					
Na			-	314	321
Ca			-	64.3	63.7
Mg			-	18.4	21.1
SO_4			-	13.0	26.0
CO_3			-	1.2	1.6
Cl			-	1.3	2.8
% water intern.			0	0	33.9
% water extern.			100	92	58.6
% water in DDL			0	8	7.5

Finally, in the third calculation we further assume that part of the water in the system is not accessible to dissolved species due to incorporation in the interlayer. The amount of water removed required to fit the analytical chloride concentration was approximately 34 %. This leads to an increase of about 60 % in chloride concentration. However, due to the effective buffering mechanisms operating in the system (see discussion in section 3.5), the other compositional changes induced by displacing the water in the interlayer are negligible.

Results referring to the reference bentonite porewater

Calculations were performed also for the conditions applying to the reference bentonite porewater (Table 3.1). Due to the considerably higher S/W ratio, larger effects of the DDL on the composition of the uncharged external water are expected. Following the scheme of the previous section, three cases where studied. The results are summarised in Table E-2.

In the first calculation, ionic segregation in the DDL was not allowed and all the water was considered to be accessible to dissolved species. This calculation corresponds thus to the main reference bentonite porewater (D-RBPW) summarised in Table 5-2, with the difference that Model 1 was applied instead of Model 2 (for the reasons mentioned earlier). As for the modelling of the Finnish experimental data it is found that the calculated porewater composition is quite insensitive to the choice of either model. Ionic strength, pH and most concentrations in solution are very similar to those calculated with Model 2. Somewhat lower Na and higher K, Mg concentrations result from the smaller selectivity coefficients assumed in Model 1 for exchange of the latter two cations with Na.

The second calculation shows the effects of including the DDL explicitly, without taking into account water displacement in the interlayers (i.e. all the water remains accessible to dissolved species as in the previous calculation). Again, we find only a small anion exclusion effect, as the equilibrium chloride concentration in the external pore water is less than 10 % higher compared to the case without DDL (the Cl molality increases from 0.168 to 0.181). Note that the fraction of DDL water is now significant (22.5 % vs. 77.5 % of uncharged external water).

Table E-2: Model calculations for the reaction between Opalinus Clay water and MX-80 bentonite at S/W= 4.5 kg L^{-1} and $pCO_2 = 10^{-2.2}$ bar.

	Initial conditions	**Model calculations (post-reaction)**		
	OPA water	**no DDL**	**with DDL, all water external**	**with DDL, 66 % interlayer water**
solution [mmol / kg H_2O]				
Na	169	236	251	482
K	5.7	2.8	3.0	5.6
Mg	7.5	8.8	9.6	25.9
Ca	10.5	13.7	14.1	27.6
Cl	160	168	181	524
CO_3	2.7	2.8	2.7	2.0
SO_4	24.0	60.0	59.0	34.5
ionic strength	0.228	0.308	0.320	0.618
pH	7.24	7.25	7.24	7.03
exch. ions [eq. fraction]	**MX-80**			
NaZ	0.848	0.832	0.839	0.866
CaZ_2	0.084	0.100	0.094	0.066
MgZ_2	0.051	0.050	0.050	0.050
KZ	0.017	0.018	0.018	0.018
CEC / eq kg^{-1}	0.787	0.787	0.787	0.787
edge sites [eq. fraction]				
$=XOH_2^+$		0.023	0.022	0.051
=XOH		0.476	0.475	0.597
$=XO^-$		0.501	0.503	0.352
net charge [meq. / kg H_2O]		-61.2	-79.1	-33.3
DDL [mmol/ kg H_2O]				
Na		-	376	559
Ca		-	28.5	39.0
Mg		-	18.6	36.2
SO_4		-	37.2	31.9
CO_3		-	2.1	1.9
Cl		-	127	479
% interlayer water		0	0	66.0
% external water		100	77.5	11.5
% water in DDL		0	22.5	22.5

In the third calculation, we study the additional effect of water incorporation in the interlayer. It was assumed that water is removed until 11-12 % of the total water is left as external solution, (in contrast to 77.5 % in the previous case). This corresponds to a residual external porosity of about 5 %, as estimated in Appendix B. Our results indicate now significant effects: with respect to the preceding calculation, the pH decreases by 0.2 units, the elemental concentrations of exchangeable cations in the external solution increase by a factor of two, the chloride concentration increases by a factor of three, whereas carbonate and sulphate concentrations are reduced. These effects are induced by the reversal of the Na-Ca exchange reaction. Due to the strong removal of external water, Na is concentrated to a level sufficient to displace exchanged Ca from the clay (in all previous cases, the opposite occurred). The displacement of Ca into the aqueous phase entrains gypsum and calcite precipitation (instead of dissolution) with consequent acidification of the solution. These results differ qualitatively from the corresponding calculation performed earlier with Model 2, where gypsum and calcite were predicted to dissolve (see section 3.5.4). These differences can be ascribed to the different Na-Ca selectivity assumed in either model. Nevertheless, the final results of the two model variants are still comparable.

Conclusions

The refined models presented in this section clearly indicate that the compositional effects induced by the explicit consideration of cation surface excesses in the diffuse double layer are generally negligible. Significant changes in the porewater chemistry are predicted only if double layer effects are assumed in conjunction with the incorporation of large amounts of water in the interlayer, at very high S/W ratios. At repository conditions ($pCO_2 = 10^{-2.2}$ bar, S/W = 4.5 kg L^{-1}) this model predicts a more concentrated bentonite porewater (I ~ 0.6 vs. ~ 0.3 molal) and a lower pH (7.0 vs. 7.25) compared to the reference composition, calculated without explicit consideration of double layer and swelling effects. The difference, however, is not important in terms of radionuclide solubilities and sorption values. In fact, the increased chloride concentration has only a minor effect on the speciation of a few radionuclides. The lower pH, on the other hand, lies within the uncertainty range (pH = 6.9 - 7.8) attributed to the conventional reference water.